Ribonucleotide reductase in anoxic and normoxic crucian carp

By Jonas Bergan

Program for Physiology

Department of Molecular Biosciences

Faculty of Mathematics and Natural Sciences

University of Oslo, 2008

Acknowledgments

First of all, I would like to thank my supervisor, Professor Göran Nilsson, for having me as his master student, and for his advices and support throughout my time as a member of his group.

I would like to thank my co-supervisor, Guro Sandvik, for being such a positive person, and for always being there whenever I needed help, encouragement, or someone to discuss with.

I would also like to thank my co-supervisor Stian Ellefsen for valuable discussions and assistance with real-time RT-PCR experiments.

A part of this project has been done in collaboration with Professor Kristoffer Andersson's group, and I am very grateful for the guidance and assistance provided by him and the members of his group, including Åsmund Røhr, Ane Tomter, and Maren Backstrøm, in the field of protein biochemistry.

I would also like to thank all the students and employees at the Program for Physiology for creating an including and stimulating environment, both scientifically and socially.

I would also like to express my gratitude to my parents, Tone and Stein, for all the support and encouragement I have received during my time as a student. A special thanks to my father for valuable feedback regrading the writing of this thesis.

Finally, I would like to thank my wonderful fiancée, Ingeborg, who is an incredibly supportive and understanding person.

Jonas Bergan

Oslo, February 2008

Table of contents

Abstract

The crucian carp (*Carassius carassius*) inhabits lakes and ponds in Northern Europe, where it is able to survive anoxia that often occurs for months during the long winter. Several physiological adaptations, including the exotic ability of ethanol production, allows the crucian carp to cover its energy needs by anaerobic metabolism, making the survival dependent on its glycogen stores.

There are several oxygen-dependent processes in animals that are not directly related to the generation of ATP. One of these is the production of DNA precursors, deoxyribonucleotides, where the radical-based enzyme ribonucleotide reductase (RNR) catalyzes the rate-limiting step of synthesis. The generation of the radical required for the catalytic mechanism is oxygen-dependent in all eukaryotes, implying that this process cannot occur in anoxic crucian carp. Nevertheless, previous studies have shown that DNA synthesis continues in crucian carp exposed to seven days of anoxia.

In this study, genes coding for the crucian carp RNR were cloned, and the expression of the subunits that constitutes the enzyme was quantified by real-time RT-PCR. Results showed that all subunits needed for RNR activity in proliferating cells were expressed in both the heart and the liver of normoxic and anoxic crucian carp. This supports the previous observations of cell proliferation in anoxic crucian carp, and the presence of the S-phase specific R2 subunit also suggests that there is mitotic activity in the crucian carp heart and liver during anoxia.

In the heart there was a significant decrease in the transcription of the R1 and p53R2 subunits in the anoxic crucian carp. As these subunits are believed to be responsible for providing deoxyribonucleotides for DNA repair and mitochondrial DNA replication, this reduction probably reflects a depressed mitochondrial activity due to the inability to maintain respiration.

The crucian carp subunits responsible for generating and storing the radical, R2 and p53R2, were purified from over-expressing *Escherichia coli* cells and investigated by electron paramagnetic resonance (EPR) spectroscopy. These experiments concluded that the chemical environment of the radical in crucian carp RNR is similar of mammalian RNR. At present, it is therefore not possible to conclude if, and explain how, this enzyme is able to function in anoxic crucian carp.

1 Introduction

Prolonged oxygen deprivation is lethal to most vertebrates. However, there are a few vertebrates that have mechanisms for overcoming the problems associated with anoxia. One of these is the crucian carp (*Carassius carassius*), a teleost inhabiting ponds and lakes in Northern Europe. Due to thick ice coverage, blocking photosynthesis and oxygen diffusion from air, these habitats may become anoxic for several months during the long winter. In such waters the crucian carp is known to be the only fish able to survive (Holopainen *et al.*, 1986). Living for longer periods without oxygen presents a multitude of problems, which all have been solved by evolution in this organism. Many of these solutions are well understood, but a lot of them clearly demand a closer investigation.

1.1 Crucian carp adaptations to anoxia

The energy crisis

All organisms are dependent on energy in the form of ATP. The most efficient way of obtaining ATP is by oxidative phosphorylation. This oxygen dependent process yields theoretically 36 moles of ATP per mole of glucose. In contrast, the anaerobic alternative, glycolysis, yields only 2 moles of ATP per mole glucose. In vertebrates, failure of maintaining ATP levels, especially in the brain and the heart, will result in loss of ion homeostasis, cell depolarization, and eventually death. There are two possible strategies for maintaining ATP levels in the absence of oxygen; to increase the rate of glycolysis, or to depress the rate of ATP use (Lutz and Nilsson, 1997). Both of these strategies are employed by the crucian carp. Nevertheless, unlike other known anoxia-tolerant vertebrates, such as several species of freshwater turtles (*Trachemys* and *Chrysemys*), the crucian carp maintains a substantial physical activity during periods of anoxia (Nilsson *et al.*, 1993).

The up-regulation of glycolysis raises certain other difficulties. Anaerobic production of ATP results in an accumulation of the end product, lactate, leading to acidosis if not removed. The crucian carp and its close relative, the goldfish (*Carassius auratus*), have solved this problem by an adaptation enabling them to convert lactate to ethanol, which in contrast to lactate, can be released through the gills (Johnston and Bernard, 1983; Shoubridge and Hochachka, 1980). Although ethanol excretion allows the crucian carp to evade one problem associated with anaerobic ATP production, glycolysis is an inefficient process compared to oxidative phosphorylation; removing

lactate as ethanol involves wasting a high-energy hydrocarbon to the surroundings. Substantial reserves of glycogen are needed to maintain the glycolytic process for longer periods. This is reflected by the crucian carp liver, which reportedly has the largest glycogen store of any vertebrate (Hyvärinen *et al.*, 1985). The liver may constitute 15% of the total body weight, with glycogen comprising as much as 30% of the liver weight. With no lactate self-poisoning it is in fact the total exhaustion of the glycogen stores that eventually limits the survival of crucian carp in anoxia (Nilsson, 1990).

Although the crucian carp is able to continue ATP production by glycolysis without suffering from acidosis caused by end-products, a reduction in ATP expenditure is necessary to prevent depletion of glycogen stores until oxygen access is regained. Energy consumption is down-regulated by metabolic depression, and it has been shown that body heat production in anoxic goldfish is reduced to about one-third (van Waversweld *et al.*, 1989). Studies from crucian carp and goldfish also reveal that in response to oxygen deprivation the activity of the central nervous system is reduced by reversible suppression of the activity of the auditory nerve (Suzue *et al.*, 1987) and retina (Johansson *et al.*, 1997). Despite the depressed metabolism the crucian carp remains physically active, although locomotion is decreased by 50-75% (Nilsson *et al.*, 1993). The maintained activity in anoxia seems to demand an active circulatory system for shuttling of substrates and end-products of glycolysis; the brain needs to be supplied with glycogen, and ethanol needs to be removed to prevent self-intoxication. This has been confirmed by observations of crucian carp retaining its normal cardiac activity and cardiovascular regulation after exposure to several days of anoxia (Stecyk *et al.*, 2004). An apparent advantage of remaining physically active during hypoxia and anoxia is to have the opportunity to seek out oxygen rather than waiting for it to arrive.

Other physiological adaptations to low oxygen availability in the crucian carp and the goldfish include hemoglobin with an extremely high affinity for oxygen, which allows maintenance of routine oxygen consumption rate in water with oxygen levels down to 5-10% of air saturation (Burggren, 1982; Sollid *et al.*, 2003). In hypoxia the ability to take up oxygen is further improved by changing the morphology of the gills (Sollid *et al.*, 2003) (Figure 1.1). In normoxia the crucian carp gills consist of lamellae covered by an interlamellar cell mass (ILCM). The morphological change observed after exposure to hypoxia consists of removal of the ILCM by apoptotic cell death, which leads to an 7.5-fold increase in the respiratory surface of the gills (Sollid *et al.*, 2003). Nevertheless, this response is only observed in hypoxia, not when the crucian carp is exposed to

anoxia (Sollid *et al.*, 2005). The reason for this may be that an increased respiratory surface does not provide an advantage unless there are some oxygen present in the water. In anoxia it actually may be a disadvantage, as exposing more of the lamellae may increase the risk of pathogens and toxic substances entering the body, as well as having undesirable osmotic effects (Nilsson, 2007). Another explanation might be that the apoptotic mechanism itself is oxygen dependent, and therefore cannot be induced in the complete absence of oxygen (Sollid and Nilsson, 2006).
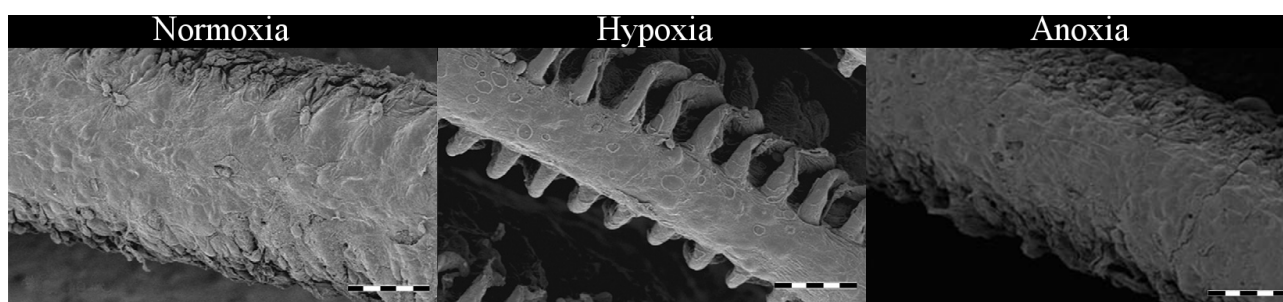
Figure 1.1: Morphological changes in crucian carp gills. After 7 days of hypoxia the respiratory surface of the gills is increased by apoptotic cell death of cells covering the lamellae. The morphological change is not observed in anoxia. Adapted from Sollid *et al.* (2005) and Sollid and Nilsson (2006).

Other oxygen-dependent processes

All adaptations to anoxia described above is related to the energy crisis caused by the oxygen dependence of cellular ATP production. There are, however, other oxygen-dependent processes not directly involved in energy metabolism, although these processes have not been subject of much investigation in anoxic crucian carp. One such process is DNA synthesis, where the production of the building blocks for DNA, deoxyribonucleotides, is oxygen-dependent in virtually all eukaryotes (Jordan and Reichard, 1998).

1.2 Ribonucleotide reductase

The enzyme ribonucleotide reductase (RNR) is responsible for the conversion of ribonucleotides to deoxyribonucleotides (Figure 1.2). Deoxyribonucleotides serve as building blocks for DNA, and the presence of functional RNR is therefore essential for synthesis and repair of DNA. This means that RNR is likely to be found in nearly all growing cells in any living organism. When reducing ribonucleotides to deoxyribonucleotides RNR employs a multi step chemical process, including a radical-based mechanism (Reichard and Ehrenberg, 1983). The RNR enzyme is responsible for the *de novo* synthesis of all of the four different deoxyribonucleotides that make up the DNA.
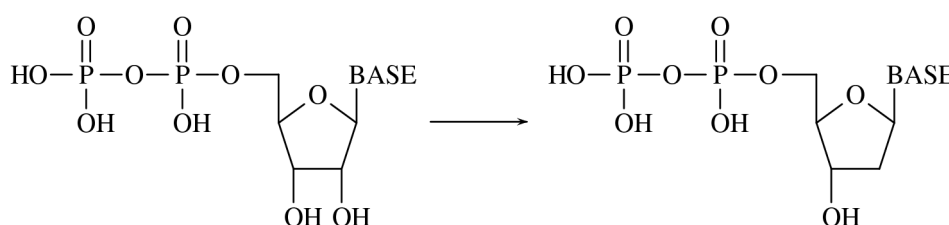
Figure 1.2: RNR converts ribonucleotides to deoxyribonucleotides. The synthesis is performed on the level of diphosphates, which subsequently are converted to triphosphates that can be utilized in DNA synthesis.

Classification

Ribonucleotide reductases are grouped into three major classes; Class I, II, and III (Jordan and Reichard, 1998; Reichard, 1993). This classification is based on the mechanisms used for radical generation and structural differences. Different metal cofactors are necessary for the enzymatic activity of the enzymes of the three classes; a diiron-oxygen cluster in Class I, cobalamin in Class II, and an iron-sulfur cluster in Class III. Still, all three classes have a conserved cysteine residue at the active site that is converted to a thiyl radical. All identified eukaryotic RNRs belong to Class I, but Class I enzymes are also found in eubacteria, bacteriophages and viruses. The generation of the radical in Class I RNRs is dependent on oxygen, and all these enzymes are therefore limited to aerobic conditions. Class II and III enzymes are found in archaea, eubacteria and bacteriophages. Class II enzymes functions independently of oxygen, while class III enzymes are strictly anaerobic as oxygen rapidly will destroy their radicals. Organisms adapted to both aerobic and anaerobic conditions may have a combination of class I and class III enzymes (e.g. *Escherichia coli*), or solely class II enzymes (e.g. *Lactobacillus*).

Only Class I enzymes are discussed in the remaining of this text, unless otherwise is indicated. *E. coli* RNR has served as a model for Class I RNR, and most of the information about the structural and functional properties of RNR is based on studies of this organism. Eukaryotic RNRs constitute a uniform group of Class I enzymes, which has been best explored in the mouse.

Structure

The active Class I RNR enzyme has a tetrameric $\alpha_2\beta_2$ structure, where α represents the large R1 protein and β represents the smaller R2 protein. The structures of the proteins have been determined by crystallography for both R1 and R2 separately in *E. coli* (Nordlund *et al.*, 1990; Uhlin and Eklund, 1994), and for R2 in mouse and human (Kauppi *et al.*, 1996; Welin *et al.*, Unpublished). However, the crystal structure of the R1-R2 holoenzyme complex has not yet been determined in any of the organisms.

The R1 protein consists of two identical subunits. In mouse the subunit has a relative molecular mass of 90 210, and is composed of 792 amino acids (Caras *et al.*, 1985; Thelander and Berg, 1986). The R1 monomer consists of three domains; a N-terminal helical domain, a central ten-stranded β/α-barrel, and a small $\alpha\beta\alpha\alpha\beta$ domain (Uhlin and Eklund, 1994). The active site, where the catalysis is performed, is located in a cleft between the N-terminal domain and the central β/α-barrel domain. The R1 subunit also contains two separate sites for allosteric regulation; one regulating overall enzymatic activity, and one regulating the substrate specificity.

The R2 protein also consists of two identical subunits. In mouse each subunit is composed of 390 amino acids and has a relative molecular mass of 44 000 (Thelander and Berg, 1986). The R2 monomer structure is mainly α-helical, and the fold of the subunit is described as three layers of helices (Nordlund *et al.*, 1990) (Figure 1.3A). Each of the R2 subunits contains a dinuclear iron center, where a stable free radical is formed in the presence of molecular oxygen. This free radical is harbored by a tyrosyl, and stabilized by the iron center (Atkin *et al.*, 1973; Reichard and Ehrenberg, 1983). In addition to its function as a radical generator, the R2 subunit has a domain in the carboxyl end necessary for the formation of the holoenzyme complex (Sjöberg *et al.*, 1987). This domain is presumed to bind to a shallow groove between two helices in the R1 subunit (Uhlin and Eklund, 1994). Although the structure of the R1-R2 enzyme has not yet been determined, a model of the holoenzyme complex has been proposed using the available R1 and R2 dimer structures (Uhlin and Eklund, 1994) (Figure 1.3B).
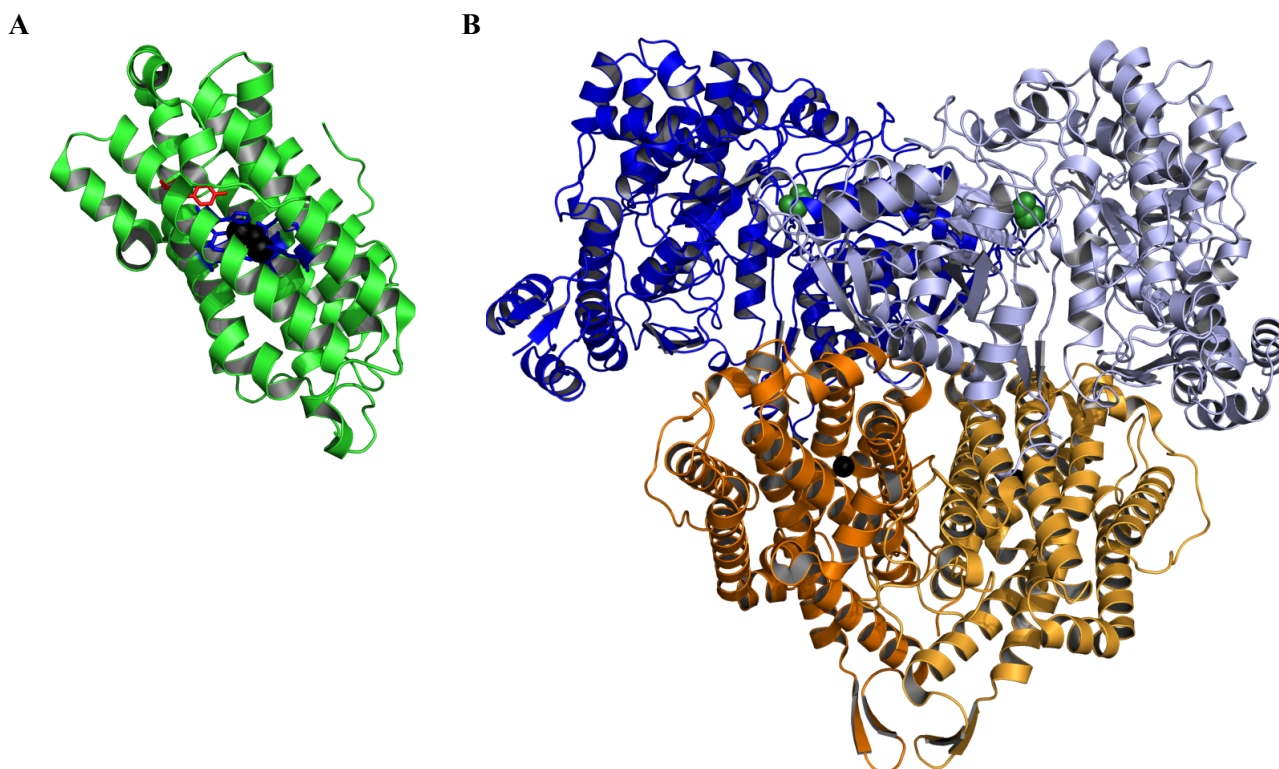
Figure 1.3: (**A**) Structure of mouse R2. The image shows the structure of the mouse R2 homodimer. In contrast to *E. coli* R2, which has a small β-hairpin, mouse R2 is exclusively α-helical. The iron site is shown in black, with surrounding iron ligands colored blue. The tyrosine harboring the radical is shown in red. The image was created from PDB-file 1W68 (Strand *et al.*, 2004) using PyMol molecular graphics software (DeLano, 2002). (**B**) Tentative structure of *E. coli* R1-R2 complex according to Eklund *et al.* (2001). The R1 dimer (blue) sits on top of the R2 dimer (orange). Each of the two active sites at the R1 subunit are marked green, while the R2 diiron sites, where the radicals are formed, are marked black. The image was created from PDB-files 1RIB (Nordlund and Eklund, 1993) and 2R1R (Eriksson *et al.*, 1997) using PyMol molecular graphics software.

Generation of the radical

The radical required for the enzymatic activity of RNR is generated in the R2 subunit, where it is stored until catalysis is initiated. Each R2 subunit can in its apo form bind two ferrous ions, giving the reduced, diferrous form of the protein. The iron binding sites are coordinated by one aspartate, two histidines and three glutamate residues, which seem to be conserved in all class I enzymes (Kolberg *et al.*, 2004). When the reduced R2 is exposed to molecular oxygen the iron center and the tyrosine residue is simultaneously oxidized to give active R2, containing diferric iron center and the stable tyrosyl radical (Figure 1.4).
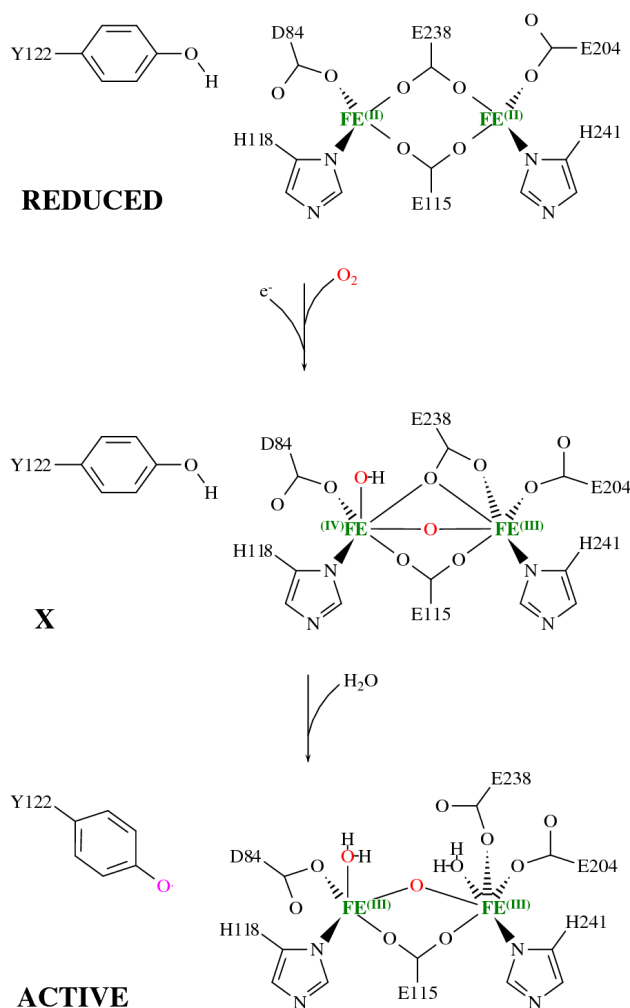
Figure 1.4: Generation of the radical in *E. coli* R2. The reduced, diferrous form of R2 is spontaneously oxidized in the presence of molecular oxygen. Through a series of intermediate states the diferric iron site and the stable tyrosyl radical (shown in pink) is generated. Only one intermediate state, X, is shown in this figure. Numbering of amino acid residues coordinating the diiron site is based on the *E. coli* structure. The figure is adapted from Kolberg *et al.* (2004)

This reaction from the apo form to active subunit requires a proton and one external electron, and can be summarized by the following (Bollinger *et al.*, 1991; Ochiai *et al.*, 1990):

$$2Fe^{2+} + Tyr-OH + O_2 + e^- + H^+ \rightarrow$$
$$Fe^{3+}-O^{2-}-Fe^{3+} + Tyr-O\cdot + H_2O$$
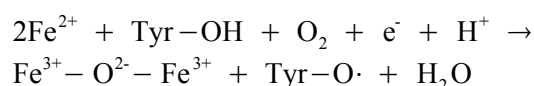
The external electron can be supplied from exogenous iron(II) (Covès *et al.*, 1997). Several reaction intermediates, known as intermediate U and intermediate X, have been identified (Bollinger *et al.*, 1991). Intermediate X contains one ferric and one ferryl ion and a normal tyrosine residue. There has also been observed two forms which can be generated *in vitro* from the active R2; a transient

mixed-valence form containing one ferric and one ferrous ion (Atta *et al.*, 1994), and a metR2 form, where the radical is scavenged by a single electron reductant (e.g. hydroxyurea), resulting in a diferric iron center and a normal tyrosine (Sahlin *et al.*, 1990).

Despite a low sequence homology (about 25%), there is a high structural similarity between eukaryotic and *E. coli* R2 proteins (Kauppi *et al.*, 1996). Still, there are some differences between the two, and one of them is found in the stability of the iron center. The iron center in mouse R2 is more labile than in *E. coli* R2, and loses 50% of its iron after 30 min at 37 °C (Nyholm *et al.*, 1993). This means that the iron-radical center of active R2 proteins in mammals has to be continuously regenerated *in vivo* in a reaction requiring ferrous iron and oxygen.

Catalytic mechanism

The conversion of ribonucleotides to deoxyribonucleotides takes place at the active site in the R1 subunit, in a mechanism requiring a radical. The RNR radical is stored deep within the R2 subunit, and therefore cannot participate directly in the reaction. Thus, a long-range transfer of the radical from the small to the large subunit is necessary (Nordlund *et al.*, 1990). A model for the catalytic process based on studies of *E. coli* RNR has been proposed (Mao *et al.*, 1992) (Figure 1.5). This model has later been supported by structural studies (Eriksson *et al.*, 1997) and experiments using site-directed mutagenesis (Persson *et al.*, 1997).
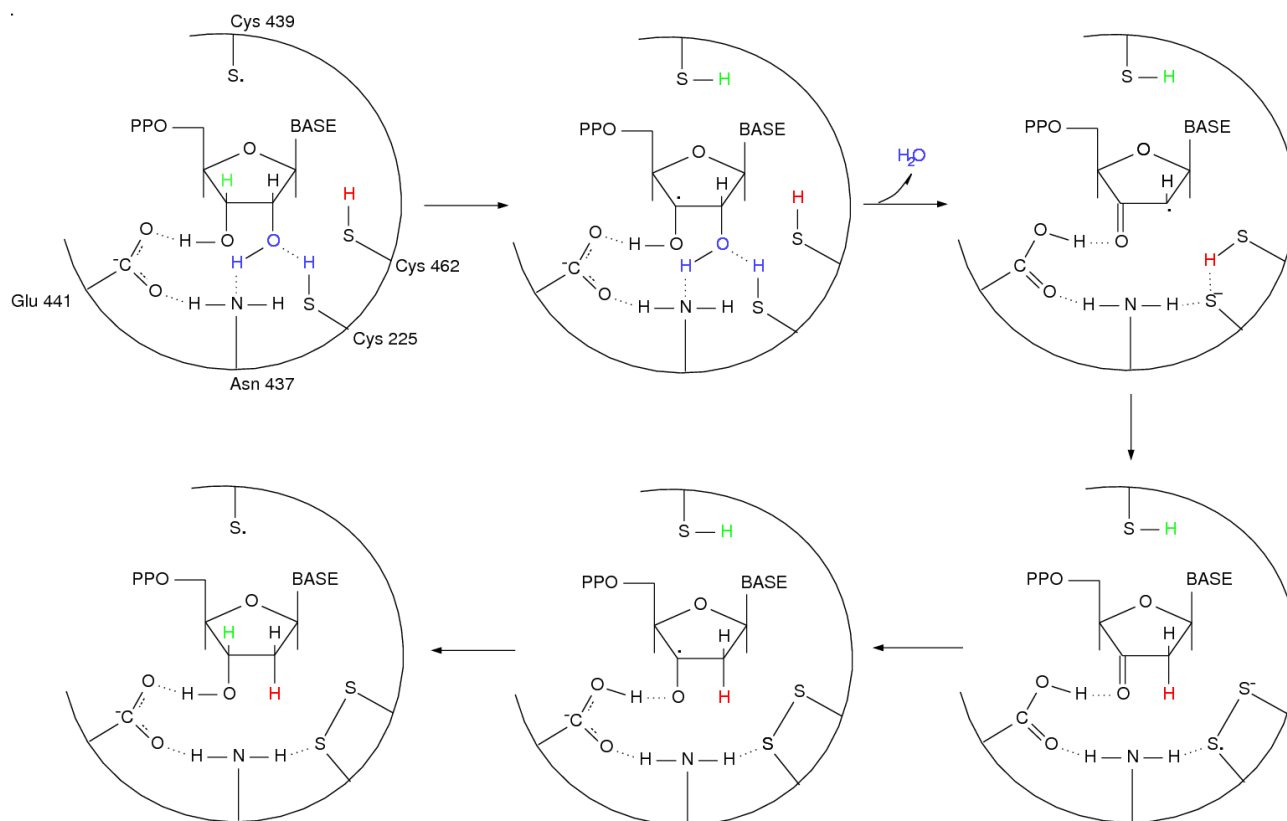
Figure 1.5: Catalytic mechanism of RNR. The figure shows the proposed mechanism of reducing ribonucleotides to deoxyribonucleotides at the R1 active site. The involved amino acids are conserved in all known class I R1, and are here shown with *E. coli* numbering. See text for details. Adapted from Kolberg *et al.* (2004).

When substrate binds to the enzyme, the radical function is transferred from the R2 tyrosyl to the active site of the R1 protein, generating a thiyl radical. This radical initiates the substrate reduction by abstracting the 3'-hydrogen atom, generating a substrate radical intermediate. This is followed by protonation of the 2'-OH-group, which eventually leaves as a water molecule. A hydrogen atom is then transferred to the 2'-position, oxidizing two cysteine residues to a disulfide anion radical. After catalysis, the thiyl radical is regenerated by returning the stored hydrogen atom to C-3', yielding the final product. The thiyl radical exists only transiently, and the radical function is transferred back to the R2 subunit where the stable tyrosyl is reformed. The oxidized sulfhydryl groups on R1 are restored by thiol coenzymes; thioredoxin or glutaredoxin (Holmgren and Aslund, 1995; Holmgren and Björnstedt, 1995). Reducing power of these coenzymes is ultimately provided by NADPH.

Regulation of activity

The amount of deoxyribonucleotides in an S-phase cell is only sufficient for a few minutes of DNA replication, and excessive amounts of deoxyribonucleotides may increase errors made by DNA polymerases. Additionally, a balanced pool of the different deoxyribonucleotides in the cell is important to ensure high quality DNA replication (Mathews and Ji, 1992; Reichard, 1988). The RNR enzyme is allosterically regulated, i.e. the activity of the enzyme is regulated by the binding of effectors. Two separate allosteric binding sites affecting both the activity and specificity of the enzyme is found in the R1 subunit (Thelander and Reichard, 1979). The general activity of RNR is regulated by the binding of either ATP (activating) or dATP (inhibitory) to the activity site (also known as the *l*-site). When active, the specificity of the enzyme is regulated by binding either dATP (or ATP), dGTP or dTTP to a specificity site (also known as the *h*-site) (Figure 1.6). When one of these end products binds to the specificity site, a conformational change occurs at the active site, altering the preference of substrate at the substrate-binding site. dCTP does not bind to the specificity site, but instead acts allosterically on the enzyme dCMP deaminase, which catalyzes the production of dTTP. At the specificity site, binding of dATP (or ATP) stimulates reduction of CDP and UDP, binding of dTTP stimulates reduction of GDP and inhibits reduction of CDP and UDP, and binding of dGTP stimulates reduction of ADP. In this way, a balanced production of the different nucleotides is ensured.
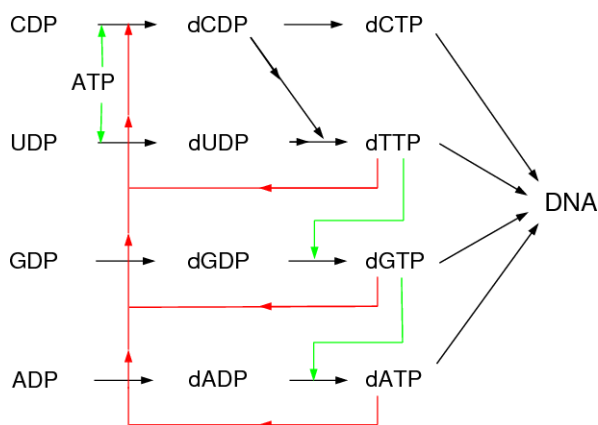
Figure 1.6: Allosteric regulation of RNR specificity. The specificity of the enzyme is regulated by the binding of effectors at the specificity site. Stimulating effects are shown in green, inhibiting effects are shown in red. In addition, ATP and dATP have stimulating and inhibitory effects, respectively, on the general activity of the enzyme by binding to a separate activity site.

As the reduction of ribonucleotides is performed on the level of diphosphates, ribonucleoside diphosphates (dNDPs) is subsequently phosphorylated to deoxyribonucleoside triphosphates

(dNTPs) in a reaction catalyzed by nucleoside diphosphate kinase, an enzyme common for all the four nucleotides. Finally, DNA contains thymine rather than uracil, and deoxythymidine triphosphate (dTTP) is produced from both CDP and UDP in several reaction steps (Reichard, 1988).

The role of RNR in replication

The supply of deoxyribonucleotides is essential for proliferating cells during the S-phase of the cell cycle, when the genomic material is duplicated. As the catalyst in the rate-limiting step of dNTP synthesis, the activity of RNR is important in regulating the kinetics of the replication (Herrick and Sclavi, 2007). The expression of RNR has shown to be cell-cycle regulated, with both activity and expression reaching a maximum during the S-phase , when the demand for deoxyribonucleotides is greatest (Björklund *et al.*, 1990; Engström *et al.*, 1985). The R1 subunit is expressed at a nearly constant level throughout the cell cycle, and the level of the active RNR enzyme complex is thereby determined by R2 levels (Engström *et al.*, 1985). The level of the R2 subunit in eukaryotic cells is regulated both transcriptionally and by enzyme degradation. R2 expression is initiated in early S-phase, leading to an accumulation in the cell until late mitosis, where the protein is subject to rapid degradation (Chabes and Thelander, 2000). This degradation is caused by the binding of a Cdh1-anaphase-promoting complex to a KEN box sequence in the R2 protein, which leads to ubiquitination and proteolysis (Chabes *et al.*, 2003).

The p53R2 subunit

A few years ago an analog of the R2 subunit was discovered in mammalian cells (Tanaka *et al.*, 2000). This protein has been named p53R2 (R2 B is also used), as the gene coding for this protein is a target for the p53 tumor suppressor. The amino acid sequence of p53R2 is very similar to regular R2, with the major difference being the lack of an N-terminal region (33 amino acids in mouse p53R2) in the p53R2 homolog (Guittet *et al.*, 2001). In mammalian p53R2 genes, the p53 binding site is located in the first intron. All functional sites are conserved, including the iron ligands, the radical site tyrosine, the amino acid residues involved in long range radical transfer, and the C-terminal sequence binding to the R1 subunit. It has been demonstrated *in vitro* that p53R2 forms a highly active RNR enzyme together with the regular R1, including the small subunit iron-tyrosyl radical center (Guittet *et al.*, 2001).

p53 is a sequence specific DNA-binding protein, acting on a number of genes involved in DNA repair, cell cycle regulation and apoptosis. Cells with deficient p53 may avoid S-phase checkpoints and possibly proliferate into a cancer. In fact, mutations in the gene coding for p53 is found in more than half of all adult human tumors (Hollstein *et al.*, 1991). Activation of the p53 protein is observed in response to DNA damage and other forms of cellular stress. When exposing mammalian cells to UV irradiation, coinciding increases in p53, R1, and p53R2 is observed (Guittet *et al.*, 2001; Tanaka *et al.*, 2000), and it has therefore been hypothesized that p53R2 is involved in synthesis of deoxyribonucleotides for DNA repair. Later studies have also revealed that p53R2 is expressed in p53 mutant cells, and that the basal transcription of the p53R2 gene is unaffected by the presence of p53 (Byun *et al.*, 2002). This has been confirmed by studies showing that p53R2 is expressed at constitutively low levels in most cells, although elevated expression may be observed in response to p53-induction (Håkansson *et al.*, 2006).

It is not only proliferating cells that require the activity of RNR; G_0/G_1-cells need to be provided with dNTPs for both DNA repair and mitochondrial DNA (mtDNA) replication. As the R2 protein is absent in these cells, salvage pathways has long been considered responsible for providing dNTPs for these processes (Arnér and Eriksson, 1995). The salvage pathway is a complementary route for providing DNA precursors, and is based on the recovery of deoxyribonucleotides from deoxyribonucleosides through the activity of several enzymes. Deoxyribonucleosides for salvage are primarily supplied through uptake from the extracellular space, and are derived from nutrients or degraded DNA. However, it is considered unlikely that nucleoside salvaging is the only way of obtaining dNTPs for DNA repair and mtDNA synthesis in resting cells, and following the discovery of p53R2 it has been proposed that p53R2-dependent *de novo* synthesis of dNTPs is involved in these activities (Håkansson *et al.*, 2006; Pontarin *et al.*, 2007). The involvement of p53R2-dependent RNR activity in mtDNA replication has been confirmed by observations of severe mitochondrial depletion in both mice and humans with mutations in the gene coding for p53R2 (Bourdon *et al.*, 2007).

The importance of p53R2 has also been illustrated by studies of p53R2-deficient mice (Kimura *et al.*, 2003; Powell *et al.*, 2005). The development of these mice appeared normal, but after six weeks the mice suffered from growth retardation and organ failures, and by 14 weeks all mice had died due to severe renal failure.

1.3 Class I RNR activity in anoxia

As the generation of the radical in class I RNR is an oxygen dependent process, it is expected that the maintenance of the dNTP pools is halted in anoxia (Thelander *et al.*, 1983). The inactivity of RNR therefore suggests that DNA synthesis is impossible in anoxia when the supply of dNTP is denied. Nevertheless, during long-term anoxia there is likely to exist a need for basic maintenance of tissue integrity, and this may involve cell proliferation and, consequently, DNA synthesis and dNTP production.

In addition, DNA in all living organisms continuously suffers from a myriad of types of damage, and failure of mechanisms repairing such damage can lead to serious disease (Friedberg, 2003). The discovery of the p53R2 protein has provided a link between RNR activity and DNA repair, and one may expect that a nonfunctional p53R2 due to the absence of oxygen will make cells more disposed to DNA damage.

This raises an interesting question regarding anoxia survival in crucian carp: Is the ability to maintain tissue integrity by cell proliferation and DNA repair lost as a consequence of nonfunctional RNR due to the lack of oxygen, or does adaptations of the RNR allow these processes to continue under anoxic conditions?

So far, one study has been conducted investigating the role of RNR in anoxic crucian carp (Sollid *et al.*, 2005). By staining new DNA through 5'-bromo-2'-deoxyuridine (BrdU)-incorporation and staining for proliferating cell nuclear antigen (PCNA) it has been shown that anoxia induces a reduction of cell proliferation in several tissues. Still, a substantial amount of proliferating cells was observed after 7 days of anoxia. In the ILCM of the gills the percentage of cells being in S-phase was reduced from 12.2% to 6.0%, while in intestinal crypts the fraction of S-phase cells went from 8.1% to 1.8%. In the liver, where only a moderate cell proliferation is seen, the amount of S-phase cells remained unchanged at approximately 1%. The same study also revealed that the expression of RNR R2 mRNA in the gills did not decrease significantly after 7 days of anoxia. These findings suggest that the crucian carp is able to maintain DNA synthesis in the absence of oxygen. If this is the case, the crucian carp must have a RNR enzyme with properties not seen in any other vertebrate.

1.4   Aims of study

This study aimed to investigate properties and expression of crucian carp RNR. This was done by identifying and characterizing transcripts coding for the various subunits of this enzyme in crucian carp. Furthermore, this information was used to quantify the expression of the different subunits in normoxia and anoxia by real time RT-PCR in two different tissues from crucian carp. This quantification was carried out in heart and liver tissues. Finally, this study aimed at using electron paramagnetic resonance (EPR) spectroscopy to investigate if there are any properties of the tyrosyl radical center in crucian carp R2 and p53R2 indicating that these proteins can sustain activity in the absence of oxygen.

2 Materials and methods

2.1 Animals

Crucian carps used in these experiments were captured in Tjernsrud pond, Bærum, Norway. They were kept in tanks (100 fish/500 l) continuously supplied with aerated and dechlorinated Oslo tap water, at the aquarium facility of the Department of Molecular Biosciences, University of Oslo. The fish were maintained on a 12:12 light-dark cycle, and fed daily with commercial fish food (TetraPond, Tetra), except during experiments.

Anoxia exposure

Anoxia exposures were performed at 8 °C, and included two exposure groups; 7 days normoxia and 7 days anoxia. Exposures were carried out in circular 25 l tanks, continuously supplied with dechlorinated, aerated/deoxygenated water (0.5-1 ml/second). De-oxygenation was achieved by N2-bubbling (Nitrogen 99.99%), and oxygen levels were monitored using a galvanometric oxygen electrode (WTW 340i from Wissenschaftlich Technische werkstätten, Germany). Fish were left to acclimate in the 25 l tanks for 12 hours prior to exposure, followed by removal of excrements and closure of tanks with tight lids.

2.2 Tissue sampling and isolation of total RNA

Tissues used in the cloning experiments were sampled from one fish. Heart and liver tissue to be used in mRNA quantification experiments were sampled from fish exposed to normoxia or anoxia. The fish was killed by cutting the spinal column, and brain, heart, liver, and intestine were dissected and snap-frozen in liquid nitrogen. While still frozen, the tissues were weighed and transfered to a tube containing TRIzol (Invitrogen). The volume of the TRIzol reagent was adjusted to 15 µl per mg tissue. The samples to be used in mRNA quantification experiments were also added an external standard gene, mw2060, on a pg-per-mg-basis. The samples were homogenized by using an electric homogenizer (Ultra-Turrax T 8, IKA), and isolation of total RNA was carried out according to the TRIzol protocol.

After isolation the quality of the extracted total RNA was evaluated by analyzing the material with a 2100 Bioanalyzer (Agilent), using the RNA 6000 Nano Lab Chip Kit (Agilent) according to

the manufacturer's protocol. This instrument separates the RNA strands in the sample by microcapillary electrophoresis. The ratios of 28S to 18S ribosomal RNA indicated high-integrity RNA. The concentration of RNA was determined by measuring light absorbance of 1:10 dilutions at 260 nm with a spectrophotometer (NanoDrop ND-1000). In addition, OD 260/280 ratio yielded values between 1.8 and 2.0 and the 260/230 ratio was above 1.8, indicating that the RNA sample was not polluted by proteins.

2.3   cDNA synthesis

To avoid contamination of genomic DNA, total RNA was treated with TURBO DNase (Ambion) according to the manufacturer's protocol prior to cDNA synthesis. A combination of oligo(dT) and random primers were used to prime the cDNA first-strand synthesis in the cloning experiments, while cDNA used in real-time RT-PCR was primed only by oligo(dT) primers. A 14 µl mixture containing 2 µg total RNA, 50 pmol oligo(dT)$_{18}$, (30 ng random primers), and 10 mM dNTP was made. The mixture was incubated at 65 °C for 5 min and then placed on ice for 1 min. 200 U Superscript III reverse transcriptase, Superscript III first-strand buffer, and DTT in a final concentration of 50 mM (all Invitrogen) were added to a total volume of 20 µl. The mixture was then incubated at 25 °C for 5 min, followed by 60 min incubation at 50 °C. The enzyme was inactivated by heating to 70 °C for 15 min. cDNA was diluted 10-fold and stored at -20 °C.

2.4   Partial cloning of RNR subunits

With the exception of a fragment of the R2 subunit (Sollid *et al.*, 2005), genes coding for crucian carp RNR have not previously been cloned. It was therefore necessary to design primers based on known RNR sequences from other species. R1, R2 and p53R2 sequences from zebrafish (*Danio rerio*), chicken (*Gallus gallus*), human (*Homo sapiens*), mouse (*Mus musculus*), rat (*Rattus norvegicus*), and African clawed frog (*Xenopus laevi*) were obtained from NCBI web resource. These sequences were aligned using ClustalW alignment software (Chenna *et al.*, 2003), and primers were designed based on the consensus sequence of these alignments. Extra attention was paid to the zebrafish sequences, as this obviously is the closest relative to the crucian carp of the species mentioned above. The primers were designed using the web-based Primer3 resource (Rozen and Skaletsky, 2000), with target melting temperature set to 60 °C. Primers in conserved regions were preferred, and the primers were made degenerate if non-conserved residues were included. For each subunit four forward primers and four reverse primers were designed. The primer sequences

are listed in Table 2.1. For each subunit each forward primer was combined with each reverse primer when setting up the PCR reactions. Primers were synthesized by Invitrogen.

Table 2.1: Primers used for cloning RNR subunits

Gene	Forward primer 5'→3'	Reverse primer 5'→3'
R1	TGGAGCGTTCATATYTGYTG	GCCTCCGTACTCTCAAABGG
	ATTGCGGCTGCWATTGAAAC	AACAGAGGCCAACTTCTBRA
	GAGCCACTGGCAGBTACATT	TTGCAAACTGCAACCTCATC
	GAGGAGCAGAGAGCCAGRGA	TCGGCACTGGTGTACTCHAC
R2	CGCTTTGTCATTTTCCCMAT	AGTCGGTCAGCCACAAACTC
	TTCTGGACAGCTGAGGAGGT	TTCATGCCAATGAGCTTHAC
	TTCCCTGAAAGACGANGAGA	GGGAAGAGCATCAGTNARGA
	GGCTTCCAGATAGCMATGGA	AGGCATGAGTCCCCKYTTCT
p53R2	GCACAGGCTTCTTTCTGGAC	TTTGTTTTCCCCTCCARNGA
	CTTTCTTTGCGGCAAGTGAT	TCCTGTTCAATKCTVACVGC
	GGTCCAGAGGTTCAGTCAGG	AGTGTAGGCCCTCRTCYCTG
	GTTCAGACCATGCCNTRTGT	GGCATCAGGCCTCTYTTCTT

A mixture of cDNA synthesized from total RNA isolated from brain, heart, liver, and intestine was used as template for the PCR. Platinum Taq DNA polymerase (Invitrogen) was used to amplify the target regions. Primers were added to a final concentration of 0.5 μM, or 1.5 μM if degenerate primers were used. The PCR was performed on a Mastercycler gradient thermal cycler (Eppendorf) using the following conditions: Initialization at 94 °C for 10 min, 42 cycles consisting of denaturation at 94 °C for 30 s, annealing at 58 °C for 30 s, elongation at 72 °C for 1 min, followed by a final elongation at 72 °C for 10 min. PCR products were ligated directly into pGEM-T Easy vectors (Promega) according to the manufacturer's protocol and transformed into CaCl$_2$-competent *E. coli* cells. Transformed cells were grown on LB plates, containing ampicillin and IPTG/X-Gal for selecting positive transformants. Several colonies from each plate were used separately as templates for colony PCR. The reaction was primed by M13 forward and reverse primers using identical conditions as described above, except for lowering the annealing temperature to 55 °C. Products from colony PCR were visualized by agarose gel electrophoresis and sequenced by the ABI-lab at CEES, Departments of Biology and Molecular Sciences, University of Oslo.

2.5 Full-length cloning by rapid amplification of cDNA ends (RACE)

RACE is a technique used to amplify ends of mRNA transcripts. Different mechanisms are utilized for 5' ends (Scotto-Lavino *et al.*, 2006b) and 3' ends (Scotto-Lavino *et al.*, 2006a), both requiring a central sequence of the transcript to be known. This technique makes it is possible to obtain full-length cDNA for mRNA transcripts where only parts of the sequence are available.

cDNA used in RACE were synthesized from mRNA purified from total RNA using Dynabeads mRNA Direct Kit (Invitrogen). This kit isolates the mRNA by using magnetic beads with covalently bound oligo(dT) sequences which hybridizes to the polyA tail of mRNA.

cDNA for 5'-RACE was synthesized using SMART RACE cDNA Amplification Kit (Clontech), according to the manufacturer's protocol. In this kit the cDNA is synthesized using oligo(dT) primer and a reverse transcriptase variant that, upon reaching the end of the mRNA template, exhibits terminal transferase activity, adding a 3-5 dC tail to the 5' end of the first-strand cDNA. A specific oligonucleotide anneals to this dC rich tail and serves as an extended template for the reverse transcriptase, which then switches templates from the mRNA molecule to the oligo. Thus, cDNA copies of the original RNA with a recognizable sequence at the 5' end is generated.

The cDNA used for 3'-RACE was synthesized using GeneRacer Kit (Invitrogen), according to the manufacturer's protocol. In this kit the cDNA is synthesized using a modified oligo(dT) primer, resulting in all cDNA copies having a recognizable 3' end that can be used as priming site in the RACE PCR.

To amplify target genes by RACE PCR gene specific primers (GSPs) based on the sequences obtained from partial cloning of RNR subunits were used. The primers were designed using Primer3 resource based on recommendations in the RACE protocols. The 5' GSP was constructed to be used with the GeneRacer 3' primer, and the 3' GSP was constructed to be used with the SMART RACE universal primer (which serves as 5' primer). Four GSPs for 3'- and 5'-RACE were designed for each of the previously cloned fragments. All GSPs used in RACE PCR are listed in Table 2.2. Primers were synthesized by Invitrogen.

Table 2.2: Primers used in RACE PCR

Gene	5'-RACE primers (5'→3')	3'-RACE primer (5'→3')
R1	CCCCAATACCTCCGGCCGACT	GCATGCCATCATTGAGTCGCAGA
	TGAGGGCGCACTGCTTCAGG	TCGCAGACAGAGACCGGAACACC
	GGAGAGCTGTGGCCGGTTGG	CCGCAAGAGCAACCAGCAGA
	TTGGTGCCGGCGTTGAACAG	CAGCAGAACCTGGGCACCATCA
R2	GCGCCCAGTCAGCCTTCTTCT	TCATGCCTGGACTCACCTTCTCCA
	GCAACGGGCTTCAGTCACTTGGA	TGCCTGCCTCATGTTCAAGCAC
	TGCCATCACTCGCAGCGAAA	CCAAGTGACTGAAGCCCGTTGCT
	GGTCAACCTCCTCTGCAGTCCAGAAA	GCCCGTTGCTTCTACGGTTTCCA
p53R2	GGCCCAGTCTGCTTTTCGCCTTA	GGCCTGATGGCTGGACTCACC
	GCTTTTCGCCTTACACAAGGCATGG	CCATCTGCTGACCGAGTGAAAGACA
	CACCTCTTGACTGAACCGCTGCAC	CACAAAAGCTGTGAGCATCGAACAGG
	GGAGCGAGCTTCTGGGATCTGCC	CGTCAATTTGATCGGGATGAACTGC

The RACE PCR was carried out using Advantage 2 Polymerase (Clontech) according to the manufacturer's protocol. The following conditions were used for the RACE PCR: Initialization at 94 °C for 10 min, 42 cycles consisting of 94 °C for 30 s, 68 °C for 30 s, 72 °C for 1 min 30 s, completed by final elongation at 72 °C for 10 min. The PCR products were then analyzed by agarose gel electrophoresis. If low product specificity (i.e. many bands) was observed, touch-down PCR was performed by lowering the annealing temperature in the following manner: Initialization at 94 °C for 2 min followed by 5 cycles of 30 s at 94 °C, 30 s at 72 °C, 1 min 30 s at 68 °C, 5 cycles of 30 s at 94 °C, 30 s at 70 °C, 1 min 30 s at 68 °C, 20 cycles of 30 s at 94 °C, 1 min 30 s at 68 °C, and finally 10 min at 72 °C. This reaction was performed using nested primers and the initial RACE product as template.

RACE products were by cloned and sequenced as previously described.

All obtained sequences are listed in appendix IV.

2.6 Quantification of mRNA expression with real-time RT-PCR

The real-time RT-PCR was conducted on a LightCycler 480 using LightCycler 480 SYBR Green I Master kit (Roche). This kit utilizes SYBR Green, which is a fluorogenic dye that binds to the minor groove of double stranded DNA, but not to single stranded DNA (Morrison *et al.*, 1998). During the real-time PCR the LightCycler is monitoring the fluorescence emitted during the reaction as an indicator of amplicon production during each cycle. The quantification of the original cDNA is done in the exponential phase of the PCR, as this is the only phase where the efficiency of the reaction is constant. By using the second derivative maximum method the LightCycler software calculates the cycle number at which the increase in fluorescence is highest, called the crossing point (*CP*). The higher the initial amount of cDNA, the sooner this cycle is reached, resulting in lower *CP* values.

The relative expression of a target gene is calculated based on the primer efficiency *E* and the *CP* value of the reaction, and is expressed in comparison to a reference gene, as described by Pfaffl (2001):

$$relative\ expression = \frac{(E^{CP})_{ref}}{(E^{CP})_{target}}$$

Primers used in real-time RT-PCR were designed based on the full-length sequences obtained from crucian carp. A minimum of two gene specific primer pairs were designed for each gene using Primer3 web resource. Primers were designed to have a melting temperature of approximately 60 °C. To avoid amplifying genomic DNA, at least one primer in each pair was designed to span exon/exon junctions. As the genomic sequence of these genes is unavailable for crucian carp, DNA sequences from zebrafish were used to predict genomic junctions between exons and introns. Intron positions have been observed to be well conserved between related species (Roy *et al.*, 2003), and it is reasonable to assume that these positions are well conserved between crucian carp and zebrafish.

All the designed primer pairs were tested in a real-time RT-PCR pilot experiment using a mixture of the cDNA to be used in the subsequent experiments. The specificity of the primer pairs was determined by investigating melting curve charts, and by analyzing the PCR products by agarose gel electrophoresis and sequencing. The melting temperature of the PCR products depends on nucleotide composition, length, and sequence, and can therefore be used to differentiate amplification products (Ririe *et al.*, 1997). Primer pairs with satisfying efficiency should therefore

yield products exhibiting a single peak in the melting curve analysis. In addition, the PCR product should result in one clear-cut band on an agarose gel and the sequence obtained by sequencing should match the known target sequence. Only primer pairs fulfilling these criteria were used in the real-time RT-PCR experiment, and these primers are listed in Table 2.3.

Table 2.3: Real-time RT-PCR primer sequences

Gene	Forward primer 5'→3'	Reverse primer 5'→3'	Efficiency
R1.1	GAGTACACCAGTAAGGATGAGGTG	GATGAAGGCATCAGCCAGAC	1.90
R1.2	GGGAGAGGAATTTGAGAAGC	CCTTACTGGTGTACTCTACAATTTCTG	1.85
R2.1	CATAAAAGATCCCAAAGAGAGAGAA	GGCAGGCAAAGTCACAGTGTA	1.91
R2.2	GGCTGACAGACTTCTGCTTG	AAAACCCCTGAGTCCAAAGC	1.98
p53R2.1	GGATTGCCCAAAGTTTTCAA	AATGAAACTGTCCCGAAAAA	1.95
p53R2.1 (alt)	GGCTTCATTCTGGACAGTCG	TGGAAATAACTTCTTGATCAACTCA	1.88
p53R2.2	GGAATATCAGAATGGTCACAAGG	TTGCTGCAAAGAAAGCCAGT	1.93
mw2060	GTGCTGACCATCCGAG	GCTTGTCCGGTATAACT	1.92

Primer pair efficiencies were determined by performing real-time RT-PCR on a series of 2-fold diluted cDNA. Each of these reactions was performed in triplicates. Dilution curves showing the threshold cycle versus the logarithm of the starting concentration were produced for each primer pair by the LightCycler software. In addition, the efficiency and standard error were calculated by the software for each primer pair. The primer efficiency E is deduced by the slope of the dilution curve according to the equation (Rasmussen, 2001):

$$E = 10^{(-1/slope)}$$

The efficiency is a measure of how much PCR product that is amplified every cycle, and will have a value between 1 (no amplification) and 2 (every PCR product is replicated). The PCR efficiencies of the primers used in the experiments are listed in Table 2.3.

The quantification of RNR mRNA in normoxic and anoxic crucian carp was performed using cDNA synthesized from mRNA isolated from heart and liver tissues from six fish of each exposure group. Each cDNA synthesis was performed in parallels. An external RNA reference gene, mw2060, was added to the tissues prior to RNA extraction on a pg-per-mg basis, allowing a more accurate normalization of data than when using internal reference genes (Ellefsen *et al.*, 2008).

For both heart and liver, the mRNA expression of each of the RNR subunits was quantified by performing four real-time RT-PCR on each fish; two reactions on each of the two cDNA syntheses.

The following program was used when performing real-time PCR: 95 °C for 10 min, 42 cycles of 95 °C for 10 s, 60 °C for 10 s, and 72 °C for 13 s. An assay for determining melting temperatures for the products was also included. This program consisted of 95 °C for 5 s and 65 °C for 10 s, followed by a gradual increase in temperature to 97 °C, where product melting temperature was measured.

Significant changes in the gene expression were tested for by using Welch's t-test. This test does not assume that the variances of the populations are equal, in contrast to the Student's t-test (Welch, 1947). The null hypothesis stating that the populations means are equal was rejected at P-values $\leq$ 0.05. In addition, two-way ANOVA was employed as a post-test, to test if the effect of exposure were the same for the different paralogs. The data sets were normality tested using the Shapiro-Wilk test. All statistical calculations were performed using MiniTab statistical software.

2.7 Expression of crucian carp R2 and p53R2 in *E. coli*

R2 and p53R2 proteins were expressed in BL21-Gold(DE3) *E. coli* cells (Stratagene) using pET-22b expression vector system (Novagen). These cells are well-suited for protein over-expression as they lack both the Lon and the OmpT protease. The cloning region of the pET-22b vector contains a T7 promoter, and can be transcribed by a T7 RNA polymerase. In the BL21 cells the T7 RNA polymerase gene is under control of a *lac* operon, and can thereby be induced by IPTG. The expression of the T7 RNA polymerase then leads to expression of the pET22b insert.

Primers for full-length cloning of R2 and p53R2 subunits were designed based on sequences obtained by RACE PCR. The primer sequences were chosen so that only the translated region of the cDNA was included in the amplified sequence. The forward primer was made complementary to region containing the start codon (ATG), while the reverse primer was made complementary to the region containing stop codon (TAG or TAA). An overhang consisting of a restriction site not present in the pET-22b vector and 3-7 additional bases was added to each of the primer sequences. The full-length primer sequences are listed in Table 2.4.

Table 2.4: Primers for full-length cloning of R2 and p53R2

Gene	Forward primer 5'→3'	Reverse primer 5'→3'
R2.2	GGAATTC<u>CAT**ATG**</u>TCGTCAACTCGCTCTC[1]	AGG<u>GTCGA**CTA**</u>AAAATCAGCATCCAGTCTG[2]
p53R2.1	GGAATTC<u>CAT**ATG**</u>GAATATCAGAACGGTCACAG[1]	AGG<u>AAGC**TTA**</u>GAAATCTGCATCGAGAGTGAA[3]

Terminal codons are highlighted in bold. Restriction sites ([1]*Nde*I, [2]*Sal*I, [3]*Hind*III) are underlined.

The products were amplified from previously synthesized cDNA using Phusion High Fidelity DNA polymerase (Finnzymes) in 50 µl reactions containing Phusion buffer, 10 mM dNTP, 0.5 µM each of forward and reverse primer and 2 µl cDNA template. The following PCR conditions were used: Initialization at 98 °C for 30 s, 35 cycles consisting of 98 °C for 8 s, 64 °C for 20 s, 72 °C for 31-35 s depending on size of target gene, and a final elongation at 72 °C for 10 min. The amplified products were analyzed by gel electrophoresis and ligated into pJET1.2 cloning vectors (Fermentas) according to the manufacturer's protocol. 2.5 µl of these reactions were used to transform $CaCl_2$ competent *E. coli* cells. Colonies from agar plates containing ampicillin were analyzed by colony PCR as described earlier, using pJET1.2 sequencing primers, and products were visualized using agarose gel electrophoresis. Positive colonies were grown in LB-medium containing ampicillin, and plasmids were isolated from cell cultures using Wizard SV MiniPrep (Promega). The purified plasmids were digested using restriction enzymes (Fermentas) corresponding to the restriction sites introduced by the PCR primers, and ligated into pET-22b expression vector using T4 DNA ligase (Promega).

Ligated plasmids were used to transform $CaCl_2$ competent BL21 cells according to the manufacturer's protocol. Transformed cells were analyzed by colony PCR and agarose gel electrophoresis, and PCR products from positive colonies were sequenced for verification, using T7 sequencing primers. Successfully transformed BL21-cells were cultured in LB-medium, added $^1/_{10}$ glycerol, and stored at -80 °C.

Cells containing R2 or p53R2 expression vectors were grown at 37 °C in 10 ml LB-medium containing 100 µg/ml ampicillin. After growing for 6 hours 5 ml of the culture was inoculated in 1 l growth medium (containing 0.9 l TB-medium, 0.1 l 1M KP_i solution and 100 µg/ml ampicillin), and incubated at 30 °C. When an optical density of 0.8-1.0 at 600 nm was observed, the culture was cooled on ice to 20 °C. The protein expression was then induced by adding IPTG to a final concentration of 1 mM. The culture was incubated at 20 °C for 12-16 hours. Samples were removed for sodium dodecyl sulfate polyacrylamide gel electrophoresis (SDS-PAGE) analysis prior to cell harvesting and prior to IPTG induction (negative control). Harvesting of cells was done by centrifugation at 6 400 x *g* for 10 min. The pellet was collected in a plastic bag, snap-frozen in liquid nitrogen, and stored at -20 °C.

SDS-PAGE was performed to verify the over-expression of the target protein. In this technique proteins are denatured by an anionic detergent (SDS), and the binding of detergent is proportional to

the mass of the protein. This gives an approximately uniform mass:charge ratio for most proteins, and the distance of migration through the gel can thereby be assumed to be directly related to the size of the protein. SDS-PAGE was performed using the Phast system (GE Healthcare), according to the manufacturer's protocol.

2.8 Protein purification

The frozen cell pellet containing over-expressed RNR were ground with a pestle in liquid nitrogen, before being disrupted by four passages through a French pressure cell (X-press, BIOX Instruments). The compressed cell material was dissolved in a solution containing 100 ml 0.1 M Tris-HCl (pH 7.5) and 5 ml 0.1 M EDTA. The sample was centrifuged at 44 000 x g at 4 °C for 1 h, and the supernatant was collected. 10% streptomycin sulfate was gradually added to the supernatant during 15 min to a final concentration of 2.5%. The sample was then centrifuged at 27 000 x g at 4 °C for 20 min, and the supernatant was collected. Ammonium sulfate was gradually added to the supernatant to a concentration of 0.39 g per ml followed by centrifugation at 15 000 x g at 4 °C for 40 min. The supernatant was removed, and the pellet was dissolved in 50 mM Tris-HCl buffer (pH 7.6) and stored at -20 °C.

To purify the protein, liquid chromatography was carried out by using Äkta Purifier System (GE Healthcare). Two methods were employed using this system; ion exchange chromatography and gel filtration chromatography.

In ion exchange chromatography proteins are separated according to differences in charge and charge distribution (Selkirk, 2003). The protein sample is transferred through a column containing a matrix with immobilized positively or negatively charged ligand groups. Columns referred to as anion exchangers contains positively charged ligands, which binds negatively charged groups, while columns referred to as cation exchangers contains negatively charged ligands, which binds positively charged groups. Elution of the proteins bound to the ion exchanger column is achieved by increasing the ionic strength of the buffer system, so that the interactions between the ligands and the charged groups are decreased by increasing the competition for the charged groups. As the proteins bound to the column usually have different affinity for the ion exchanger, gradually increasing the ionic strength of the eluent will cause elution at different times.

In gel filtration chromatography molecules are separated according to their size (Cutler, 2003). The column material is composed of small spherical particles with pores, and the probability that a

molecule will penetrate the particles varies with the size of the molecule. Smaller molecules will enter more of the pores than the longer molecules, and thereby have a longer traveling distance. This result in larger proteins being eluted before smaller proteins or other molecules.

When performing ion exchange chromatography, too high ion strength in the protein solution will prevent the proteins from binding to the column material. In order to reduce the ion strength in the protein solution, salt was removed from the solution using a desalting column. A desalting column is essentially a gel filtration column with pore sizes too small for most proteins to enter. Thus, smaller molecules, such as salts, will enter the pores, while the larger molecules, such as proteins are eluted in the solvent used to equilibrate the column. This buffer change was achieved using 2x5 ml HiTrap desalting columns (GE Healthcare), which are packed with Sephadex G-25 size exclusion medium. The columns were equilibrated with 2 column volumes of 50 mM Tris-HCl buffer (pH 7.6), before applying the sample containing the ammonium sulfate precipitated proteins. Fractions absorbing light at 280 nm were collected.

Anion exchange chromatography was performed using 2x5 ml HiTrap Q HP columns (GE Healthcare). The columns were equilibrated with 50 mM Tris-HCl buffer (pH 7.6), and samples were applied in volumes of 2 ml, The proteins that bound to the columns were eluted by linearly increasing the salt concentration. Thus, over a volume of 35 ml, the equilibration buffer was gradually changed to a buffer containing 50 mM Tris-HCl buffer (pH 7.6) and 300 mM KCl. The eluted proteins were fractionated according to their 280 nm light absorbance, and these fractions were analyzed by SDS-PAGE. Fractions containing proteins of the expected size were concentrated by ultra filtration at 5 500 x *g* for 20 min, using Amicon Ultra-15 centrifugal filter units (Millipore) with a cut-off value of 30 kDa.

Gel filtration chromatography was performed using a 24 ml Superdex 200 HR 10/300 column (GE Healthcare). The column was equilibrated with 100 mM Tris-HCl buffer (pH 7.6), and samples were applied in volumes of 50 µl. Fractions were collected, analyzed by SDS-PAGE, and concentrated by ultra filtration as described above.

Protein concentrations were calculated using the extinction coefficient previously determined for mouse R2 (Mann *et al.*, 1991). Absorption at 280 nm was measured and the concentration of protein in the sample was calculated using the Beer-Lambert law:

$$C = \frac{A}{\epsilon \times l}$$

where C is the concentration, A is the absorbance, ε is the molar extinction coefficient, and l is the sample path length.

2.9   Reconstitution of proteins

The reconstitution of the diiron-oxygen cluster and the tyrosyl radical of the R2 and p53R2 proteins was done according to a previously established procedure (Røhr, 2001), where an aerobic acidic ferrous solution is added to the protein sample. A low pH prevents loss of the ferrous ions due to oxidation, but does not appreciably lower the pH of the protein solution. The ferrous solution was prepared by dissolving ammonium iron(II)sulfate in mqH$_2$O adjusted to pH 2.3 by adding concentrated sulfuric acid. Light absorption spectroscopy was performed before and after adding the ferrous solution. When measuring the light absorption of successfully reconstituted R2 proteins a small peak at approximately 410 nm will normally be observed (Brown *et al.*, 1969).

In addition to the active form of R2/p53R2, a reduced mixed valence form of both of these proteins was prepared. This was achieved by adding phenazine methosulfate (PMS) and dithionite (DT) to the reconstituted samples (Atta *et al.*, 1994). PMS acts as an electron transfer mediator and DT as a reductant and this will reduce the proteins to the mixed valence form ($Fe^{2+}Fe^{3+}$). The mixed valence samples were prepared by adding 20% glycerol, PMS and DT to samples of reconstituted R2/p53R2, both of the latter reagents to final concentrations of 1.65 mM.

2.10 Electron paramagnetic resonance (EPR) spectroscopy

EPR spectroscopy is a technique used to detect magnetic moments of unpaired electrons in radicals and metal ions (Palmer, 2000; Symons, 1978), and it has been widely used to study the radical center of RNR R2 proteins (Gräslund and Sahlin, 1996).

The spin angular momentum of an electron is defined by its spin quantum number, m_s. The spin quantum number may have a value of $m_s = +\frac{1}{2}$ or $-\frac{1}{2}$. When an external magnetic field is applied to a atom or molecule with an unpaired electron, the spin of this electron may align either in the same ($m_s = -\frac{1}{2}$) or in the opposite ($m_s = +\frac{1}{2}$) direction of the field, a phenomenon called the Zeeman effect. Each of the two alignments corresponds to a specific energy state, $E_{-1/2}$ and $E_{1/2}$, which are described by:

$$E_{1/2} = \frac{1}{2} g \beta B$$

$$E_{-1/2} = -\frac{1}{2} g \beta B$$

where g is the electron g-factor, β is the Bohr magneton, and B is the magnitude of the magnetic field. The energy difference ΔE between these two energy levels can then be described as a function of the applied magnetic field:

$$\Delta E = E_{1/2} - E_{-1/2} = g \beta B$$

If the electron is provided with the radiation energy corresponding to the energy between the levels, the electron can jump between the two energy levels. This is known as resonance. For this "flipping of spin" the quantum of energy provided, $h\nu$, must be equal to the separation in energy between the spin states, as described by an equation referred to as the resonance condition:

$$h \nu = \Delta E = g \beta B_R$$

where h is Planck's constant and ν is the frequency of the microwave radiation. B_R is the intensity of the magnetic field which satisfies the resonance condition. It is the microwave radiation absorbed or emitted by electrons moving from one electronic spin state to another that is detected in EPR spectroscopy. Usually, an EPR spectrum recorded as the 1st derivative of the absorption. As implied by the equation above, resonance is achieved by a combination of magnetic field frequency and intensity satisfying the resonance condition. In practice, EPR spectroscopy is performed using a

fixed frequency while varying the intensity of the magnetic field. By increasing the magnetic field the energy between the $m_s = \pm\frac{1}{2}$ states increases until they match the energy of the microwaves. Typically, EPR is performed using frequencies around 9 GHz (known as X-band EPR), but higher frequencies such as 35 GHz (Q-band) and 95 GHz (W-band) are also used for increased resolution (Andersson *et al.*, 2003).

A requirement for observing an EPR signal is that the two energy states are unequally populated. If there is no population difference the rate of excitation and the rate of stimulated emission will be equal, and the net absorption will be zero. The population difference is described by the Boltzmann distribution and is dependent on the separation of the energy levels ΔE and the temperature T:

$$\frac{N_{upper}}{N_{lower}} = e^{\frac{-\Delta E}{k_b T}}$$

where N_{upper} and N_{lower} are the populations of the upper and lower energy levels, and k_b is the Boltzmann constant. As stated by this equation, the population difference is inversely proportional to the temperature, and to ensure that this difference is detectable, EPR spectroscopy is therefore often performed at cryogenic temperatures.

The spin angular momentum of an electron is characterized by the electron spin *g*-factor, also called the spectroscopic splitting factor. The *g*-value measures the rate of divergence of the $m_s = \pm\frac{1}{2}$ levels in a magnetic field. This value is anisotropic, i.e. it is orientation-dependent, having three principal values, g_x, g_y, and g_z, along three orthogonal lines. If the electron is the only source of magnetism the *g*-value is isotropic; $g_e = 2.0023$. The presence of local magnetic fields produced by nearby nuclei or electrons in the molecule adds to, or subtracts from, the spin magnetism, and this will cause deviations from the free-spin value. Thus, the electron *g*-value is determined by the immediate surroundings of the unpaired electron, and the spin-orbit coupling will give information about the nature of the molecular orbital containing the electron. The magnetic interactions between the unpaired electron and nearby magnetic nuclei in the molecule are called hyperfine couplings. Each nucleus with nuclear spin *I*, will split the signal into $2I + 1$ hyperfine lines, which may provide important structural information.

EPR samples were prepared by adding 160 µl of samples containing reconstituted R2/p53R2 proteins in a 100 µM or higher concentration to EPR tubes of 250 x 3.8 mm dimensions (outer

diameter). Tubes were immediately placed on liquid nitrogen, where they were stored until performing the EPR spectroscopy.

X-band EPR was performed using a Elexys 560 spectrometer with a ER4116DM dual mode resonator cavity (Bruker). The temperature was regulated using an ESR900 Liquid Helium control system (Oxford Instruments), allowing temperatures from 3.6 K to 100 K. Instrumental parameters are listed in Table 2.5. Experiments were performed at the EPR Laboratory, Department of Physics, University of Oslo.

Table 2.5: X-band EPR instrumental parameters

Parameter	Description	Value
Frequency	Microwave frequency	9.67 Ghz
Power	Microwave power	200 nW – 200 mW
Sweep width	Magnetic field sweep range	0 – 5000 G
Center field	Midpoint of the magnetic field	0 – 5000 G
Resolution	Number of data points collected	1024
Receiver gain	Amplification of detector signal	2×10^3 - 1×10^6
Modulation frequency	Frequency which the magnetic field is modulated	100 kHz
Modulation amplitude	Amplitude of the field modulation	3 – 5 G
Modulation phase	Detection phase of the detector	90 degrees
Conversion time	Time to convert analog voltage to digital value	163.84 - 327.68 ms
Time constant	Time to filter the analog signal	1.28 ms
Sweep time	Time to record spectrum	167.77 s
Harmonic	Selection between first or second derivative detection mode	First

3 Results

3.1 Cloning of the RNR subunits

Coding sequences of RNR subunits in crucian carp were obtained by cloning techniques. Information from the available sequences from zebrafish were used to identify fragments of the target sequences, and RACE PCR was employed to obtain full-length sequences. The obtained sequences revealed that in crucian carp there are two paralogs of each of the RNR subunits. This difference in the number of gene variants between crucian carp and zebrafish is often seen, and can probably be explained by a whole-genome duplication event occurring after their respective subfamilies, *Cyprininae* and *Danioninae*, diverged (Leggatt and Iwama, 2003). In this text the different variants are distinguished by a suffix (.1 or .2) following the name of the, e.g. R1.1 and R1.2 for the R1 subunits.

R1

Two paralogs of the crucian carp R1 were identified. The open reading frame of both of the variants consists of 2 382 bp, corresponding to a translated product of 783 amino acid (aa) residues. In class I R1 there are 80 residues conserved in more than 80% of all of the known sequences (Eklund *et al.*, 2001), including known functionally important sites in the protein. All of these residues are also conserved in both of the sequences obtained from crucian carp (Figure 3.1). The two crucian carp R1 paralogs are highly similar: 94% similarity in the nucleotide sequence and 96% similarity in the amino acid sequence.

```
Cc R1.1  MHVIKRDGRQERVMFDKITSRIQKLCYGLNAEFVDPTHITMKVIQGLYSGVTTVELDTLA
Cc R1.2  MHVIKRDGHQERVMFDKITSRIQKLCYGLNAEFVDPTQITMKVIQGLYSGVTTVELDTLA
Dr R1    MHVIKRDGGQEGVMFDKITSRIQKLCYGLNSDFVDPTQITMKVIQGLYSGVTTVELDTLA
Mm R1    MHVIKRDGRQERVMFDKITSRIQKLCYGLNMDFVDPAQITMKVIQGLYSGVTTVELDTLA
         1........10........20........30........40........50........

Cc R1.1  AEISATLTTKHPDYAILAARIAVSNLHKETKKVFSEAMEDLYNYVNPLNDRHSPMVSKET
Cc R1.2  AEITATLTTKHPDYAILAARIAVSNLHKETKKVFSEVMEDLYNYVNPLNGHHSPMISKET
Dr R1    AETAATSTTKHPDYAILAARIAVSNLHKETKKVFSEVMEDLYNYVNPLNSRHSPMISKET
Mm R1    AETAATLTTKHPDYAILAARIAVSNLHKETKKVFSDVMEDLYNYINPHNGRHSPMASST
         61......70........80........90........100.......110.......

Cc R1.1  LDIVLANKDRLNSAIIFDRDFSYNFFGFKTLERSYLLKINGKVAERPQHMLMRVSVGIHK
Cc R1.2  LDIVLANKDRLNSAIIFDRDFSYNFFGFKTLERSYLLKINGKVAERPQHMLMRVSVGIHK
Dr R1    LDIVLANKDRLNSAIIYDRDFSYNFFGFKTLERSYLLKINGKVAERPQHMLMRVSVGIHK
Mm R1    LDIVMANKDRLNSAIIYDRDFSYNYFGFKTLERSYLLKINGKVAERPQHMLMRVSVGIHK
         121......130.......140.......150.......160.......170.......
```

cont.

```
Cc R1.1   EDIAAAIETYNLLSEKWFTHASPTLFNAGTNRPQLSSCFLLAMKDDSIDGIYDTLKQCAL
Cc R1.2   EDIAAAIETYNLLSEKWFTHASPTLFNAGTNRPQLSSCFLLAMKDDSIEGIYDTLKQCAL
Dr R1     EDIAAAIETYNLLSEKWFTHASPTLFNAGTNRPQLSSCFLLAMKDDSIEGIYDTLKQCAL
Mm R1     EDIDAAIETYNLLSEKWFTHASPTLFNAGTNRPQLSSCFLLSMKDDSIEGIYDTLKQCAL
          181.....190......200......210......220......230........

Cc R1.1   ISKSAGGIGVAVSCIRATGSYIAGTNGNSNGLVPMLRVYNNTARYVDQGGNKRPGAFAMY
Cc R1.2   ISKSAGGIGVAVSCIRATGSYIAGTNGNSNGLVPMLRVYNNTARYVDQGGNKRPGAFAMY
Dr R1     ISKSAGGIGVAVSCIRATGRYIAGTNGNSNGLVPMLRVNNNTARYVDQGGNKRPGAFAMY
Mm R1     ISKSAGGIGVAVSCIRATGSYIAGTNGNSNGLVPMLRVYNNTARYVDQGGNKRPGAFAIY
          241.....250......260......270......280......290.......

Cc R1.1   LEPWHFDIFDFLELKKNTGKEEQRARDLFYALWIPDLFMKRVETNGDWCLMCPNDCPGLD
Cc R1.2   LEPWHFDIFDFLELKKNTGKEEQRARDLFYALWIPDLFMKRVETNADWSLMCPSDCPGLD
Dr R1     LEPWHFDIFDFLELKKNTGKEEQRARDLFYALWIPDLFMKRVETNGDWSLMCPNDCPGLD
Mm R1     LEPWHLDIFEFLDLKKNTGKEEQRARDLFFALWIPDLFMKRVETNQDWSLMCPNECPGLD
          301.....310......320......330......340......350........

Cc R1.1   ECWGEEFENLYTKYEKEGKAKRVVKAQQLWHAIIESQTETGTPYMLYKDACNRKSNQQNL
Cc R1.2   ECWGEEFEKLYMKYEQEGRAKRVVKAQQLWYAIIESQTETGTPYMLYKDACNRKSNQQNL
Dr R1     ECWGEEFEKLYAKYEQEGRAKRVVKAQQLWYAIIESQTETGTPYMLYKDACNRKSNRQNL
Mm R1     EVWGEEFEKLYESYEKQGRVRKVVKAQQLWYAIIESQTETGTPYMLYKDSCNRKSNQQNL
          361.....370......380......390......400......410........

Cc R1.1   GTIKCSNLCTEIVEYTSKDEVAVCNLASVALNMYVTPERTFDFQKLASVTKVIVKNLNKI
Cc R1.2   GTIKCSNLCTEIVEYTSKDEVAVCNLASIALNMYVTPERTFDFQKLASVTKVIVKNLNKI
Dr R1     GTIKCSNLCTEIVEYTSADEVAVCNLASIALNMYVTSERTFDFQKLASVTKVIVKNLNKI
Mm R1     GTIKCSNLCTEIVEYTSKDEVAVCNLASLALNMYVTPEHTYDFEKLAEVTKVIVRNLNKI
          421.....430......440......450......460......470.......

Cc R1.1   IDINYYPVQEAENSNKRHRPIGIGVQGLADAFILMRFPFESAEAQLLNTQIFETIYYAAL
Cc R1.2   IDVNYYPVREAENSNKRHRPIGIGVQGLADAFILMRFPFESAEAQLLNTQIFETIYYAAL
Dr R1     IDINYYPVKEAENSNKRHRPIGIGVQGLADAFILMRFPFESTEAQLLNTQIFETIYYAAL
Mm R1     IDINYYPIPEAHLSNKRHRPIGIGVQGLADAFILMRYPFESPEAQLLNKQIFETIYYGAL
          481.....490......500......510......520......530........

Cc R1.1   ESSCELAAEFGPYETYAGSPVSKGILQYDMWDKTPTDLWDWEALKEKIAKHGVRNSLLLA
Cc R1.2   ESSCELAAECGPYETYAGSPVSKGILQYDMWEKTPTDLWDWAALKEKITKHGVRNSLLLA
Dr R1     ESSCELAAEYGPYQTYAGCPVSKGILQYDMWEKTPTDLWDWAALKEKIANDGVRNSLLLA
Mm R1     EASCELAKEYGPYETYEGSPVSKGILQYDMWNVAPTDLWDWKPLKEKIAKYGIRNSLLIA
          541.....550......560......570......580......590........

Cc R1.1   PMPTASTAQILGNNESIEPYTSNIYTRRVLSGEFQIVNPHLLKDLTERGLWNEEMKNQLI
Cc R1.2   PMPTASTAQILGNNESIEPYTSNIYTRRVLSGEFQIVNPHLLKDLTERGLWNEEMKNQLI
Dr R1     PMPTASTAQILGNNESIEPYTSNIYHRRVLSGEFQIVNPHLLKDLTERGLWNEEMKNQII
Mm R1     PMPTASTAQILGNNESIEPYTSNIYTRRVLSGEFQIVNPHLLKDLTERGLWNEEMKNQII
          601.....610......620......630......640......650........

Cc R1.1   AQNGSIQGIPTIPDDLKELYKTVWEISQKTILKMAADRGAFIDQSQSLNIHIAEPNYGKL
Cc R1.2   AQNGSIQAIPTIPDDLKELYKTVWEISQKTILKMAADRGAFIDQSQSLNIHIAEPNYGKL
Dr R1     AQNGSIQTIPAIPDDLKELYKTVWEISQKTILKMAADRGAYIDQSQSLNIHIAEPNYGKL
Mm R1     ACNGSIQSIPEIPDDLKQLYKTVWEISQKTVLKMAAERGAFIDQSQSLNIHIAEPNYGKL
          661.....670......680......690......700......710.......

Cc R1.1   TSMHFYGWKQGLKTGMYYLRTKPAAANPIQFTLNKEKLKETQKSASNE-EEIKELNMAAMV
Cc R1.2   TSMHFYGWKQGLKTGMYYLRTKPAAANPIQFTLDKEKLKETQESTSNE-EETKERNKAAMV
Dr R1     TSMHFYGWKQGLKTGMYYLRTKPGANPIQFTLNKEKLKETQKTTSSEDEETKERNKAAMV
Mm R1     TSMHFYGWKQGLKTGMYYLRTRPAANPIQFTLNKEKLKDKEKALKEE--EEKERNTAAMV
          721.....730......740......750......760......770........

Cc R1.1   CSLENRDECLMCGS
Cc R1.2   CSLENRDECLMCGS
Dr R1     CSLENRHECLMCGS
Mm R1     CSLENREECLMCGS
          781.....790..
```

Figure 3.1: Alignment of R1 amino acid sequences in crucian carp (Cc), zebrafish (Dr), and mouse (Mm). Residues are shaded according to their similarities. The important functional sites are highlighted: active site residues (blue), radical transport residues (green), and thioredoxin interacting residues (red).

R2 and p53R2

Two paralogs of the R2 subunit were also identified. The length of the two transcripts differed by three nucleotides, giving lengths of 1 155 bp (385 aa) and 1158 bp (386 aa) for R2.1 and R2.2 respectively. The two paralogs showed a similarity of 94% in the nucleotide sequence, and 95% in the amino acid sequence.

As with the other subunits, two paralogs of p53R2 were identified. p53R2 in mammals is slightly shorter than regular R2, and this was also the case with the crucian carp ortholog. The length of the p53R2.1 transcript was 1 011 bp (337 aa), while the length of the p53R2.2 transcript was 1 047 bp (349 aa). The difference in size between the two variants is caused by a mutation in the sequence of p53R2.1 corresponding to the start codon in p53R2.2 and zebrafish, excluding 36 bases from the 5'-end of the predicted translated region. The similarity between the p53R2.1 and p53R2.2 is 94% in the nucleotide sequence, and 96% in the amino acid sequence. The similarity between the crucian carp R2 and p53R2 subunits is 75-79% on the amino acid sequence level, which is slightly lower than the similarity observed in mammals (80%) (Tanaka *et al.*, 2000).

In addition to the described paralogs, what seems to be an alternative splice variant of the p53R2.1 paralog was observed. This alternative transcript includes an 81 bp sequence not seen in the other obtained sequences. The position of this 81 bp sequence coincides with the position of a 104 bp intron in the genomic sequence from zebrafish. This implies that the transcript contains an intron, which in the "standard" p53R2.1 is removed by exon splicing. However, this intron sequence contains a stop codon, reducing the open reading frame to 348 bp, corresponding to a 116 aa translated product. It seems unlikely that this truncated p53R2.1 variant yields an functional R2 subunit, as the sequence reveals that both tyrosine radical site and most of the iron ligands are lacking.

Except for the alternative variant described above all R2 and p53R2 paralogs contain all conserved residues known to be involved in radical formation and transfer, including the tyrosyl radical site, the amino acids serving as iron ligands, and the amino acids involved in the transfer of the radical to the R1 protein (Figure 3.2).

```
Cc R2.1      MQSTRSPL--KTKNENTISAKINNMSLVDKENTPPSLSSSRILASKTARKIFD-SEEQT-
Cc R2.2      MSSTRSPL--KTKNENAVFAKMTNMSLVDKENTPPSLSSTRILASKTARKIFDDSEDQT-
Dr R2        MSSTRSPL--KTKNENTISTKMNNMSFVDKENTPPSLSSTRILASKTARKIFDESEGQS-
Mm R2        MLSVRTPLATIADQQLQLSPLKRLTLADKENTPPTLSSTRVLASKAARRIFQDSAELES
Cc p53R2.1   ------------------------------------------------MEYQNGH
Cc p53R2.2   -----------------------------------------MNSSTSNTLSSVMEYQNGH
Dr p53R2     -----------------------------------------MNSCTSNTPTVITGYQNGH
Mm p53R2     --------------------------------------MGDPERPEAARPEKGEQLCSE
             1........10........20........30........40........50.......

Cc R2.1      -KAKGAVEEEPLLKENPHRFVIFPIQYHDIWQMYKKAEASFWTAEEVDLSKDLQHWDSL
Cc R2.2      -KARKGAVEEEPLLKDNPHRFVIFPIQYHDIWQMYKKAEASFWTAEEVDLSKDLQHWDSL
Dr R2        -KAKKGAVEEEPLLKENPHRFVIFPIQYHDIWQMYKKAEASFWTAEEVDLSKDLQHWDSL
Mm R2        KAPTNPSVEDEPLLRENPRRFVVFPIEYHDIWQMYKKAEASFWTAEEVDLSKDIQHWEAL
Cc p53R2.1   RHVDTNSVEDEPLLRENPKRFVIFPIQYPDIWKMYKQAQASFWVEEVDLSKDLVHWDSL
Cc p53R2.2   KDVDANSVEDEPLLRENPKRFVIFPIQYPDIWKMYKQAQASFWTVEEVDLSKDLVHWDSL
Dr p53R2     KDVDPNSVEDEPLLRENPKRFVIFPIQYPDIWKMYKQAQASFWTVEEVDLSKDLTHWDGL
Mm p53R2     TEENVVRSNEEPLLRKSSRRFVIFPIQYPDIWRMYKQAQASFWTAEEVDLSKDLPHWNKL
             61.......70........80........90........100.......110.......

Cc R2.1      KDEERYFISHVLAFFAASDGIVNENLVERFTQEVQVTEARCFYGFQIAMENIHSEMYSLL
Cc R2.2      KDEERYFISHVLAFFAASDGIVNENLVERFTQEVQVTEARCFYGFQIAMENIHSEMYSLL
Dr R2        KDEERYFISHVLAFFAASDGIVNENLVERFTQEVQVTEARCFYGFQIAMENIHSEMYSLL
Mm R2        KPDERHFISHVLAFFAASDGIVNENLVERFSQEVQVTEARCFYGFQIAMENIHSEMYSLL
Cc p53R2.1   KSEEKHFISHVLAFFAASDGIVNENLVQRFSQEVQIPEARSFYGFQILIENVHSEMYSML
Cc p53R2.2   KSEEKHFISHVLAFFAASDGIVNENLVQRFSQEVQIPEARSFYGFQILIENVHSEMYSML
Dr p53R2     KSEEKHFISHVLAFFAASDGIVNENLVQRFSQEVQLPEARSFYGFQILIENVHSEMYSML
Mm p53R2     KSDEKYFISHILAFFAASDGIVNENLVRFSQEVQVPEARCFYGFQILIENVHSEMYSLL
             121......130......140.......150.......160.......170.......

Cc R2.1      IDTYIKDPKEREFLFNAIETMPCVKKKADWALNWIGDKNAQYGERVVAFAAVEGIFFSGS
Cc R2.2      IDTYIKDPKERDFLFNAIETMPCVKKKADWALNWIGDKNAQYGERVVAFAAVEGIFFSGS
Dr R2        IDTYIKDSKEREFLFNAIETMPCVKKKADWALNWIGDKNARYGERVVAFAAVEGIFFSGS
Mm R2        IDTYIKDPKEREYLFNAIETMPCVKKKADWALRWIGDKEATYGERVVAFAAVEGIFFSGS
Cc p53R2.1   INTYIRDLKERDYLFNAIHTMPCVRRKADWALQWISDTNSTFGERLVAFAAVEGIFFSGS
Cc p53R2.2   INTYIRDLKERDFLFNAIHTMPFVRRKADWALQWISDTNSTFGERLVAFAAVEGIFFSGS
Dr p53R2     INTYIRDLKERDYLFNAVQTMPCVRRKADWALQWISDTNSTFGERLVAFAAVEGIFFSGS
Mm p53R2     IDTYIRDPKKREFLFNAIETMPYVKKKADWALRWIADRKSTFGERVVAFAAVEGIFFSGS
             181......190......200.......210.......220.......230.......

Cc R2.1      FASIFWLKKRGLMPGLTFSNELISRDEGLHCDFACLMFKHLVNKPSEATVKKIIMNAVEI
Cc R2.2      FASIFWLKKRGLMPGLTFSNELISRDEGLHCDFACLMFKHLVNKPSEETVKKIIVNAVAI
Dr R2        FASIFWLKKRGLMPGLTFSNELISRDEGLHCDFACLMFKHLINKPSEETVKKIIMNAVEI
Mm R2        FASIFWLKKRGLMPGLTFSNELISRDEGLHCDFACLMFKHLVHKPAEQRVREIITNAVRI
Cc p53R2.1   FAAIYWLKKRGLMAGLTYSNELISRDEGLHCNFACLLYSYLVKKPSADRVKDIITKAVSI
Cc p53R2.2   FAAIYWLKKRGLMPGLTYSNELISRDEGLHCNFACLMYSYLVKKPSADRVKDIITKAVSI
Dr p53R2     FAAIYWLKKRGLMPGLTYSNELISRDEGLHCNFACLIYSYLVKKPSVDRVNDIIAKAVSI
Mm p53R2     FAAIFWLKKRGLMPGLTFSNELISRDEGLHCDFACLMFQYLVNKPSEDRVREIIADAVQI
             241......250......260.......270.......280.......290.......

Cc R2.1      EQEFLTDALPVKLIGMNCDLMKQYIEFVADRLLLELGFDKVYKVENPFDFMENISLEGKT
Cc R2.2      EQEFLTDALPVKLIGMNCDLMKQYIEFVADRLLLELGFDKVYKVENPFDFMENISLEGKT
Dr R2        EQEFLTDALPVKLIGMNCDLMKQYIEFVADRLLLELGFDKVYRVENPFDFMENISLEGKT
Mm R2        EQEFLTEALPVKLIGMNCTLMKQYIEFVADRLMLELGFNKIFRVENPFDFMENISLEGKT
Cc p53R2.1   EQEFLTEALPVNLIGMNCSLMKQYIEFVADRLLMDLGLPKVFKSENPFDFMESISLEGKT
Cc p53R2.2   EQEFLTEALPVNLIGMNCSLMKQYIEFVADRLLTDLGLPKVYKSENPFDFMESISLEGKT
Dr p53R2     EQEFLTEALPVNLIGMNCSLMKQYIEFVADRLLTDLGLPKAYCSENPFDFMESISLEGKT
Mm p53R2     EQEFLTEALPVGLIGMNCVLMKQYIEFVADRLLGELGFSKIFQAENPFDFMENISLEGKT
             301......310......320.......330.......340.......350.......

Cc R2.1      NFFEKRVGEYQRMGVMSGPTDNTFRLDADF
Cc R2.2      NFFEKRVGEYQRMGVMSGSTDNTFRLDADF
Dr R2        NFFEKRVGEYQRMGVMSGTTDNTFTLDADF
Mm R2        NFFEKRVGEYQRMGVMSNSTENSFTLDADF
Cc p53R2.1   NFFEKRVGEYQRLGVMSNVMDCEFTLDADF
Cc p53R2.2   NFFEKRVAEYQRLGVMSNVMDCEFTLDADF
Dr p53R2     NFFEKRVAEYQRLGVMSNVKDCEFTLDADF
Mm p53R2     NFFEKRVSEYQRFAVMAETTDNVFTLDADF
             361......370......380.......
```

Figure 3.2: Alignment showing the similarity of the R2 and p53R2 amino acid sequences in crucian carp (Cc), zebrafish (Dr) and mouse (Mm). Residues are shaded according to their similarity. All known functional sites are conserved in all sequences, and have been highlighted using the following code: radical site = blue, iron ligands = red, residues involved in radical transport = green.

Sequence homology

Generally, the RNR proteins of crucian carp show high sequence similarity to sequences from other vertebrates. All paralogs of both subunits are virtually equally similar to the zebrafish orthologs, while when comparing mouse and crucian carp sequences R1 is more conserved than the R2 and p53R2 sequences. The similarity of these proteins is summarized in Table 3.1.

Table 3.1: Similarities of crucian carp RNR subunits

RNR subunit	Paralogs	Zebrafish	Mouse
R1.1	96%	93%	89%
R1.2		94%	89%
R2.1	95%	96%	81%
R2.2		94%	81%
p53R2.1	96%	94%	80%
p53R2.2		93%	80%

The relatedness of crucian carp R1 and R2/p53R2 to RNR proteins of several other species is illustrated in Figure 3.3.
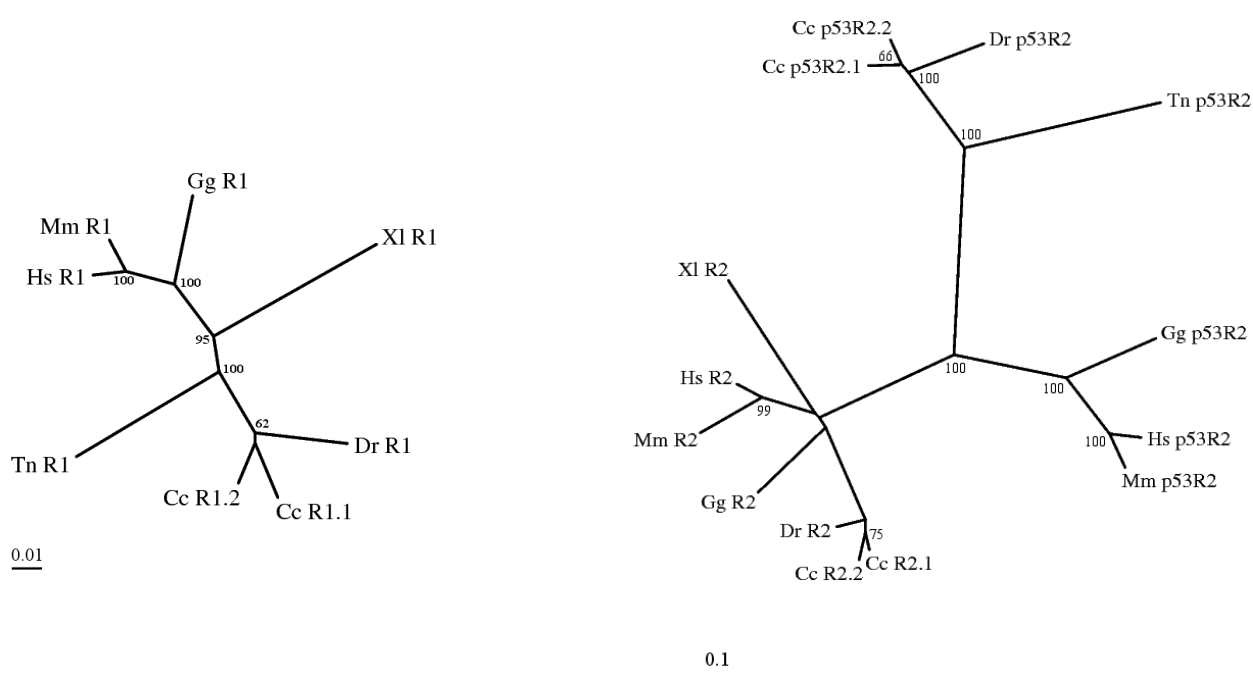

Figure 3.3: Phylogeny of RNR proteins. Unrooted phylogenetic trees showing the relatedness of RNR proteins in selected species; Cc = crucian carp, Dr = zebrafish, Gg = chicken, Hs = human, Mm = mouse, Tn = green spotted pufferfish, Xl = African clawed frog. The confidence scores (in %) of a bootstrap test of 300 replicates are indicated for branch nodes scoring over 50%. The scale bars represents estimated amino acid substitutions per site (note that the values are different for the two trees). The trees were made using Phylip phylogenetic software (Felsenstein, 1989).

3.2 Relative quantification of RNR expression in normoxia and anoxia

The expression of the identified subunits was quantified by real-time RT-PCR. This was performed using total RNA isolated from heart and liver tissues of crucian carps exposed to normoxic and anoxic conditions. mRNA levels of the various subunits were normalized to an external standard gene, mw2060.

R1

The R1 paralogs were expressed in both heart and liver tissues. In the heart significant decreases in the expression of both paralogs were observed in the anoxic exposure group (Figure 3.4), while in the liver the R1 paralogs were expressed at similar levels in both normoxic and anoxic fish (Figure 3.5). In the heart there was also a significant difference between the levels of R1.1 and R1.2 ($P = 0.004$) when performing a two-way ANOVA with paralogs and exposure as factors. There were no significant differences in the effect of anoxia on the different paralogs.
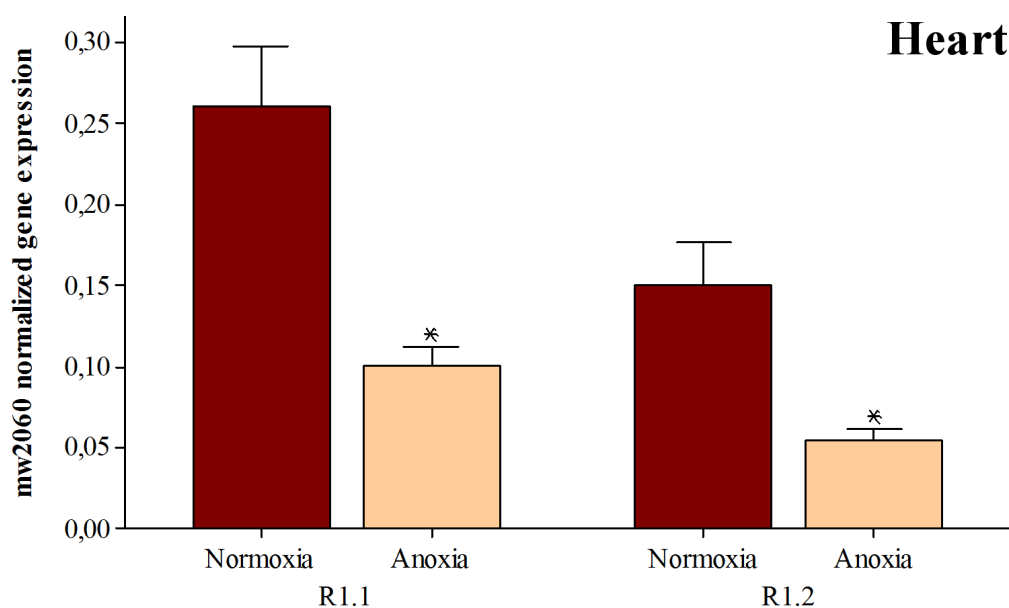
Figure 3.4: R1 mRNA expression in the crucian carp heart. Real-time RT-PCR experiments showed a significant reduction in the expression of both of the R1 paralogs in the heart tissues of anoxic crucian carp ($P = 0.010$ for R1.1 and $P = 0.018$ for R1.2). mRNA levels are expressed as mean±standard deviation, relative to the external standard. n = 6 for each group.
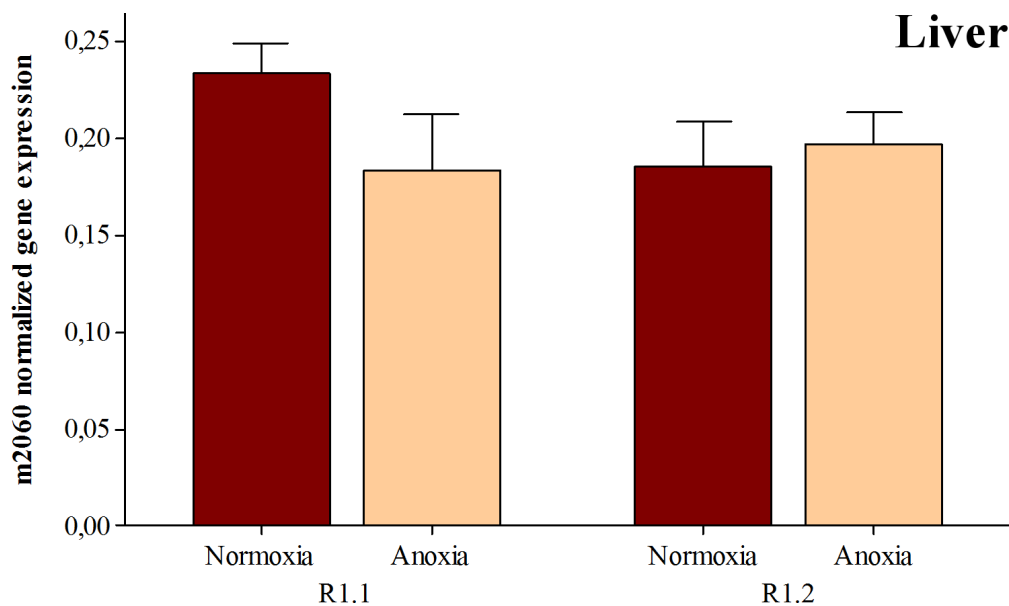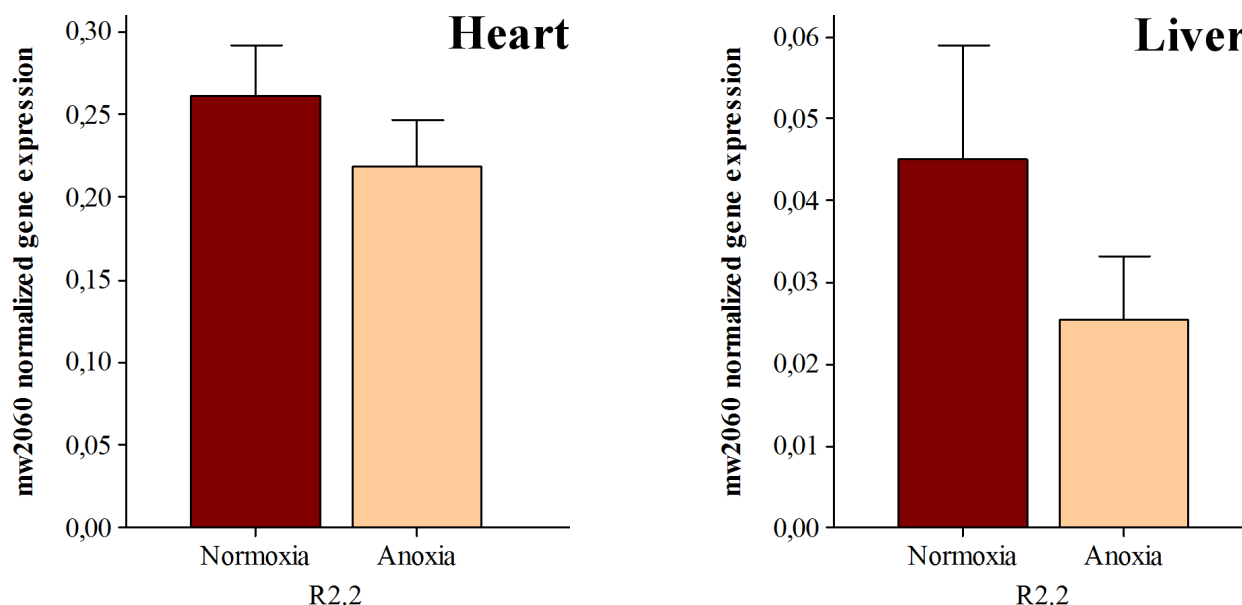
Figure 3.5: R1 mRNA expression in crucian carp liver. In the liver no significant difference between normoxic and anoxic fish was observed. mRNA levels are expressed as mean±standard deviation, relative to the external standard. n = 6 for each group.

R2

Of the two R2 paralogs, the R2.2 variant was substantially more expressed than the R2.1 variant in both heart and liver, and the *CP*-values obtained from the amplification of R2.1 were too high for quantifying the expression of this transcript using this assay. For R2.1 several observations of *CP*-values above 37 were made, while the R2.2 was detected at *CP*-values of ±27. Rather than attempting to optimize the assay for a precise quantification of the expression of R2.1, it was concluded that the levels of this transcript were substantially lower than the levels of R2.2 mRNA.

The expression of R2.2 did not change significantly in anoxia in neither of the tissues (Figure 3.6). However, the R2.2 mRNA levels in liver seemed substantially lower than in the heart when comparing to the levels of both the external standard and the R1 paralogs.
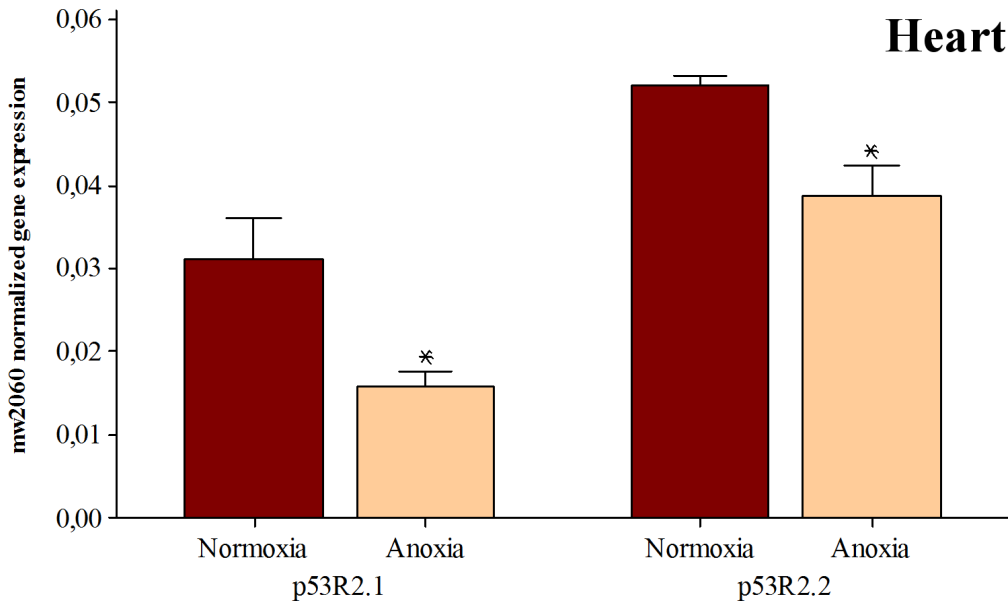
Figure 3.6: R2 mRNA expression in crucian carp heart and liver. There was no significant difference in R2 expression between the two exposure groups in neither heart or liver tissues. R2.2 levels seemed to be lower in liver than in heart when comparing the levels with the external standard and the R1 paralogs. mRNA levels are expressed as mean±standard deviation, relative to the external standard. n = 6 for each group.
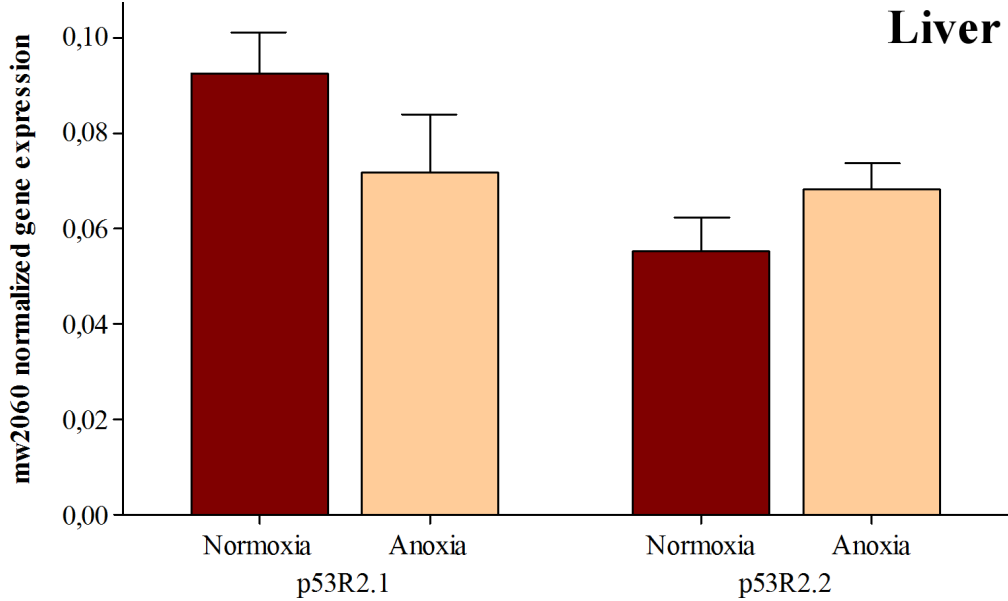
p53R2

Both p53R2 paralogs were expressed in the heart and liver from both exposure groups. In the heart, a significantly lower expression of both paralogs were observed in the anoxic group (Figure 3.7). When comparing the two paralogs, p53R2.2 levels were higher than p53R2.1 levels in heart tissue from both the normoxic and anoxic individuals ($P < 0.001$). In liver, the p53R2 paralogs showed no significant difference in expression between the two exposure groups (Figure 3.8).

Quantification of the expression of the alternative splice variant of p53R2.1 was also attempted, but low levels of this gene prevented precise quantification. It was therefore concluded that the levels of this variant were substantially lower than the other variants.

Figure 3.7: Expression of p53R2 mRNA in crucian carp heart. The expression of both p53R2.1 and p53R2.2 decreased significantly in heart tissues from the anoxic group ($P = 0.031$ for p53R2.1 and $P = 0.016$ for p53R2.2). In liver no significant change in expression was observed. mRNA levels are expressed as mean ±standard deviation, relative to the external standard. n = 6 for each group.


Figure 3.8: Expression of p53R2 mRNA in crucian carp liver. In liver no significant change in expression was observed. mRNA levels are expressed as mean±standard deviation, relative to the external standard. n = 6 for each group.

3.3 *In vitro* studies of crucian carp R2 and p53R2 proteins

After having quantified the expression of RNR subunits in two different tissues in normoxia and anoxia, one of the variants of each R2 and p53R2 was chosen to be expressed, purified, and studied by EPR. As R2.2 levels were observed to be substantially higher than R2.1 levels in both normoxia and anoxia, R2.2 was used in these experiments. Both p53R2 paralogs were expressed synchronously in heart and liver, and p53R2.1 was chosen to be used in further studies.

**Expression and purification of R2 and p53R2 proteins**

R2.2 and p53R2.1, were expressed in *E. coli* cells and purified using liquid column chromatography, and fractions obtained were evaluated using SDS-PAGE (Figure 3.9).
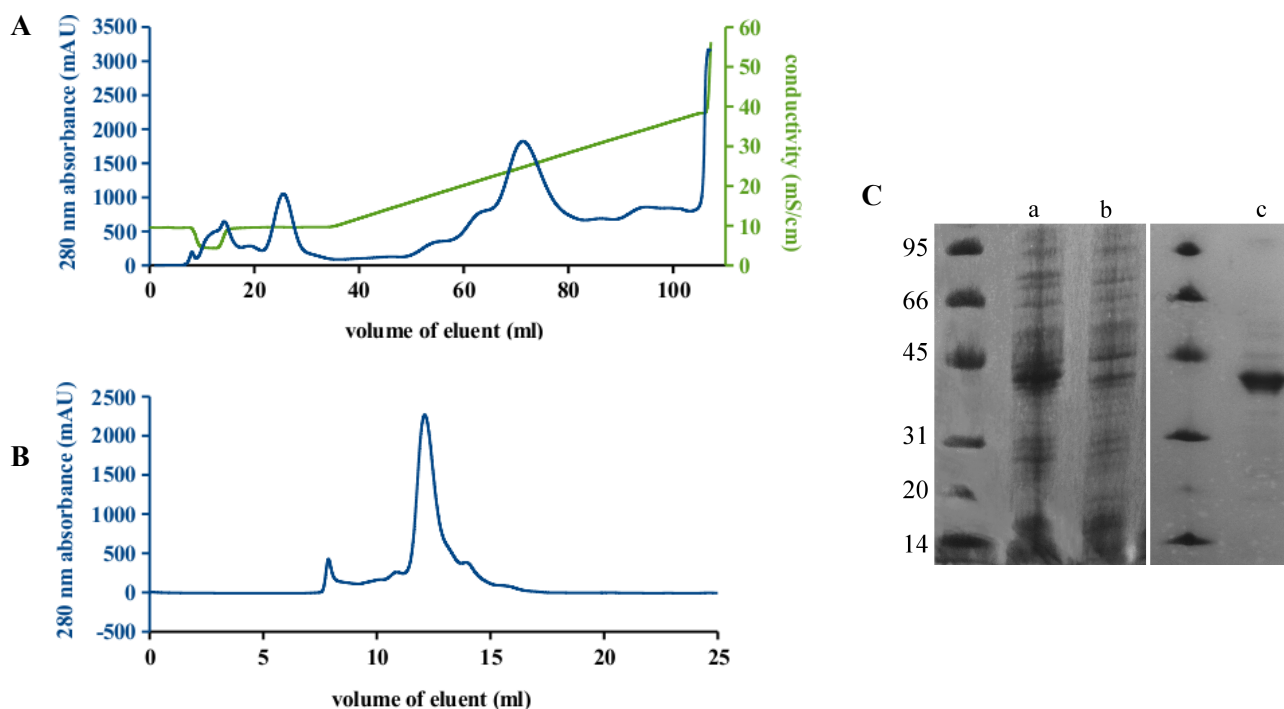
Figure 3.9: (**A**) Protein purification using liquid chromatography. Proteins were purified using anion exchange chromatography. The R2 chromatogram shows the absorbance at 280 nm (blue) and the conductivity (green), which was gradually increased by increasing the salt concentration in the eluent. The protein eluted at approximately 25 mS/cm. (**B**) Proteins were further purified by gel filtration chromatography. The peaks in the absorbance at 280 nm represents proteins of different sizes eluted at different volumes. (**C**) SDS PAGE gel showing the R2 sample before (a) and after (c) purification. The gel on the left also includes a negative control (b) where the over-expression of R2 in the *E. coli* cells has not been induced. The numbers on the left represents the relative molecular weights of the proteins in the low-molecular weight standards.

Reconstitution of the proteins

After purification the proteins were reconstituted by adding iron. The color of the protein solution then changed from weakly yellowish to green, and the absorption spectra of the reconstituted proteins showed a small peak at ~410 nm (Figure 3.10). This peak originates from a vibronic progression of a 1500 cm^{-1} C-O vibration of the tyrosyl radical, and indicates a successful reconstitution of the protein. This peak was observed for both the purified proteins.
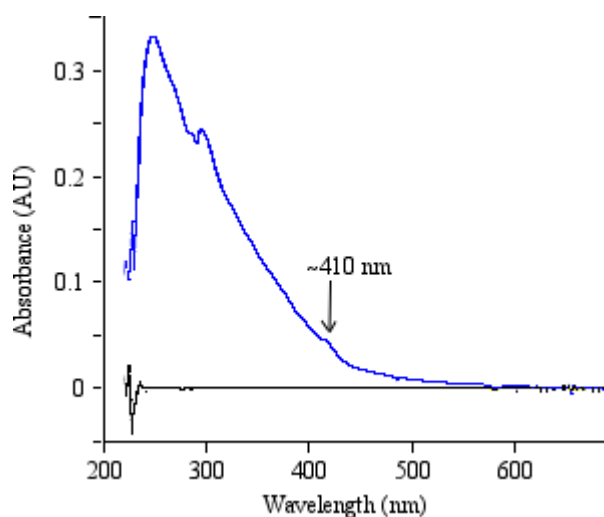
Figure 3.10: Light absorption spectrum of R2.2. The spectrum shows the difference in absorption between the reconstituted protein (blue line) and the apo protein (black baseline). The small peak at approximately 410 nm indicates the presence of a radical. Charge transfer transitions between the ferric ions and the oxygen bridge in the protein also leads to an increase in absorption in the 300-450 nm region. A similar spectrum was observed for p53R2.

EPR spectroscopy

EPR spectroscopy can be used to study the electrostatic environment of the tyrosyl radical in RNR (Andersson *et al.*, 2003). Observations of different *g*-values for the tyrosyl radical is due to variations in hydrogen bonding. Even small changes in the environment may affect the *g*-values, and different values have been observed for R2 and p53R2 proteins of different organisms. The EPR-spectrum of the R2 tyrosyl radical is generally characterized by a hyperfine splitting due to a localization of spin-density on the C_1-atom, and the dominant part of this hyperfine coupling comes from one of the β-protons. The magnitude of this hyperfine coupling is known to be determined by the dihedral angle of these β-protons.

Low temperature X-band EPR spectroscopy was performed for both R2.2 and p53R2.1. The obtained EPR spectra revealed that both crucian carp R2 and p53R2 show great resemblance to their mammalian counterparts (Figure 3.11).
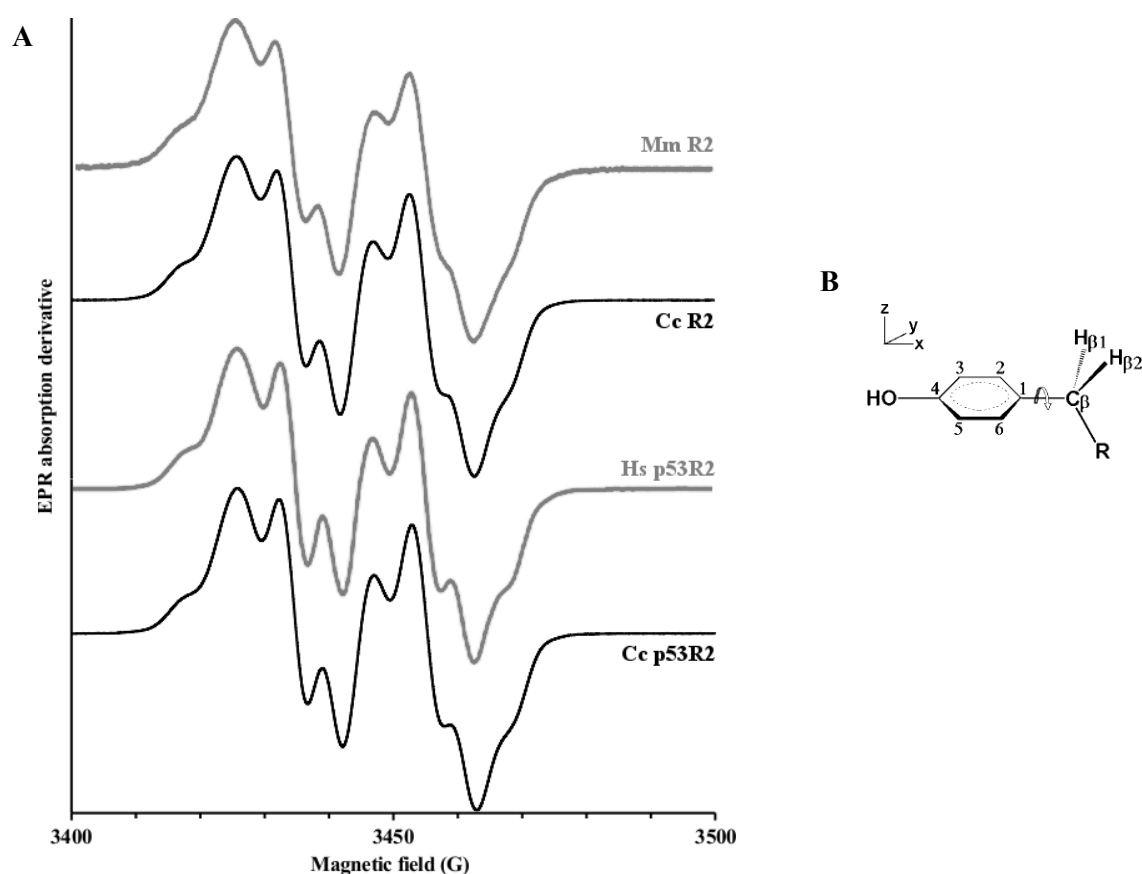
Figure 3.11: (**A**) EPR spectra of crucian carp R2 (Cc R2) and p53R2 (Cc p53R2) in the active state. Spectra were obtained at following conditions: temperature = 20 K, frequency = 9.67 GHz, and microwave power = 3 mW. Corresponding spectra of mouse R2 (Mm R2) and human p53R2 (Hs p53R2) are included for comparison (Tomter, 2006). (**B**) The hyperfine coupling is influenced by the dihedral angle of the β-protons. From Svistunenko and Cooper (2004).

The overall shape of the tyrosyl radical signal showed that both the *g*-values, line widths and hyperfine splittings are similar to active mouse and human R2 and p53R2, indicating that the chemical environment of the tyrosyl radical is the same. By simulation of the obtained spectra, the *g*-values of the active crucian carp R2 was estimated to $g_1 = 2.0080$, $g_2 = 2.0046$, and $g_3 = 2.0020$. These values are close to previously determined values for mouse R2: $g_1 = 2.0076$, $g_2 = 2.0044$, $g_3 = 2.0021$ (Bleifuss *et al.*, 2001).

Mixed valence samples of the two proteins were also prepared. This was done by treating reconstituted protein with PMS and DT, which reduces the active protein to the mixed valence state. These samples were then analyzed using X-band EPR spectroscopy (Figure 3.12). *g*-values were estimated to $g_1 = 1.92$, $g_2 = 1.73$, $g_3 = 1.61$ for crucian carp R2, and $g_1 = 1.91$, $g_2 = 1.72$, $g_3 = 1.60$ for crucian carp p53R2. These values are very similar to the ones observed in mammalian R2 (1.92, 1.73, 1.60) and p53R2 (1.90, 1.72, 1.60) (Atta *et al.*, 1994; Tomter, 2006), indicating that the structure of the diiron center in the crucian carp subunits bear a strong resemblance to the structure seen in the mammalian subunits.
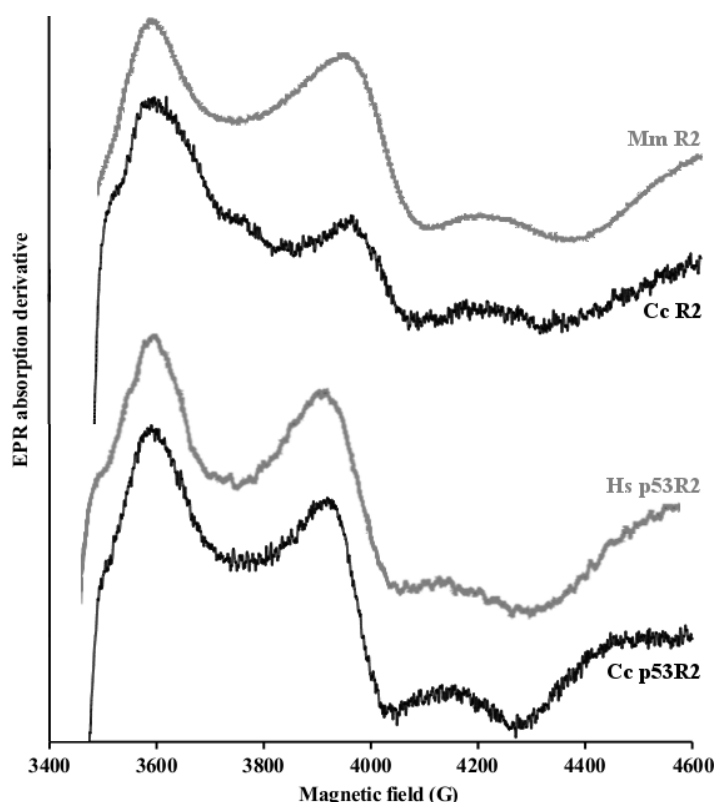
Figure 3.12: EPR spectra of crucian carp R2 (Cc R2) and p53R2 (Cc p53R2) in the mixed valence state. Spectra were obtained at temperature = 5 K, frequency = 9.67 GHz, and microwave power = 0.4 mW. Corresponding spectra of mouse R2 (Mm R2) and human p53R2 (Hs p53R2) are included for comparison (Tomter, 2006).

4 Discussion

Two paralogs each of RNR subunits R1, R2 and p53R2 in crucian carp were identified and cloned. All genes were found to be transcribed in both heart and liver during both normoxia and anoxia. The expression of all of the genes was quantified, except R2.1, which was expressed at substantially lower levels than the other genes, and therefore mRNA levels could not be determined precisely. In heart, R1 and p53R2 were expressed at significantly lower levels in fish exposed to 7 days of anoxia than in normoxic fish, while R2 levels were not significantly affected by anoxia. In liver, there were no significant differences in the expression of any of the RNR subunits when comparing normoxic and anoxic fish.

4.1 Real time RT-PCR considerations

The usage of an external control enables comparison of the effect of different treatments (e.g. anoxia) without having to rely on assumptions that some genes (i.e. internal reference genes) are constitutively expressed and unaffected by the experimental treatment (Ellefsen *et al.*, 2008). One should, however, be cautious when comparing the relative expression of a gene across different tissues, as the efficiency of the RNA extraction and the presence of inhibitory factors altering the PCR efficiency may vary between the tissues (Tichopad *et al.*, 2004; Wilson, 1997). The results of the relative quantification of gene expression presented here are therefore mainly evaluated by comparing the levels of a gene in one tissue at a time.

One weakness of quantifying mRNA levels is that these do not necessarily reflect the abundance of proteins produced in the cell (Gygi *et al.*, 1999). Still, it seems pointless for an organism facing an energy crisis to waste energy on producing unneeded mRNA transcripts. It has been shown that protein synthesis is reduced in a tissue-specific manner in anoxic crucian carp, and both in the heart and the liver the process is heavily depressed (53% and >95%, respectively) during anoxia (Smith *et al.*, 1996). Further investigations indicated that this occurs without corresponding reductions in the levels of total RNA synthesis (Smith *et al.*, 1999). However, the translatable mRNA constitutes only a few percent of the total RNA synthesized.

4.2   RNR in proliferating cells

In mammals, it has been shown that the expression of R1 and R2 proteins is mainly regulated at the transcriptional level (Björklund *et al.*, 1990). However, there are also observations of R2 protein levels varying independently of transcript levels (Eriksson *et al.*, 1984), suggesting that the expression also may be partially regulated at the post-transcriptional level. In mammals the R2 gene has two promoters, which produces two major mRNAs with 5'-untranslated regions (5'-UTRs) of different lengths (Dong *et al.*, 2005), and it has been suggested that these UTRs of mRNA may act as *cis* elements in a translational control of the transcript. The obtained 5'-UTRs of the crucian carp R2 are very different from human and mouse R2, so it remains unclear if this post-transcriptional mechanism is conserved across these species. Nevertheless, this translational regulation is only considered to contribute to the fine-tuning of the protein expression, while the principal regulation occurs at the transcriptional level. Thus, one might expect that the levels of mRNA transcript and protein correlates in crucian carp, as they do in mammals, and that the R1 and R2 mRNA expression reflects the abundance of the corresponding proteins.

Studies of mammalian cells have shown that the levels of R1 and R2 proteins are significantly elevated in proliferating cells; in quiescent or terminally differentiated cells the levels of proteins are very low or undetectable (Engström *et al.*, 1985; Mann *et al.*, 1988). The mammalian R1 protein in proliferating tissues is expressed at relatively constant levels throughout the cell cycle, with a half life of approximately 15 h (Engström *et al.*, 1985). In contrast, the expression of mammalian R2 has shown to be strictly S phase correlated, with a short half life of only 3 h (Eriksson *et al.*, 1984). The R1 expression has therefore been characterized as proliferation-specific, while the expression of R2 is considered cell cycle-specific and responsible for regulating the RNR activity during cell division. The fact that these proteins normally is seen only in proliferating cells makes it reasonable to assume that the R1 and R2 mRNA transcripts presently detected in crucian carp heart and liver originate from proliferating cells. Thus, the results also suggest that there is cell proliferation in both these tissues in anoxia.

The observed expression of R1 and R2 in anoxic heart and liver is consistent with previous observations of cell proliferation in anoxic crucian carp (Sollid *et al.*, 2005). In crucian carp liver the amount of proliferating cells have been determined to 1%, and this fraction is maintained after exposure to 7 days of anoxia (Sollid *et al.*, 2005).

There are currently no data on anoxic cell proliferation available for the crucian carp heart. In mammalian hearts cell proliferation is virtually absent (Ahuja *et al.*, 2007). However, in zebrafish a high level of proliferating cardiomyocytes has been observed in response to heart injury (Poss *et al.*, 2002). In uninjured zebrafish hearts, 3% of the cells incorporated BrdU during a 7-day labeling period, and in regenerating hearts more than 30% of the cells were BrdU-labeled 14 days after the injury. This mitotic activity is high compared to mammals, and most likely reflects the fact that fishes and their hearts continue to grow throughout life. The fact that the proliferation-specific RNR proteins R1 and R2 were found to be expressed in the crucian carp heart indicate a considerable cardiomyocyte cell cycle activity also in the crucian carp, and that this is maintained in anoxia. This obviously needs to be confirmed by more specific studies of mitotic activity.

The results of the relative quantifications presented here also indicate that the R2 levels relative to both R1 and the external standard are substantially higher in the heart than in the liver. This may suggest that the amount of proliferating cells is in fact higher in the heart than in the liver, perhaps corresponding to the levels reported in zebrafish.

The expression of R2.2 has previously also been quantified in normoxic and anoxic crucian carp gills (Sollid *et al.*, 2005), where no significant differences between the exposure groups were detected. These observations are consistent with the observations of R2 transcript levels in heart and liver tissues presented in this study.

In heart, there was a reduction of about 60% in R1 expression during anoxia, while R2 mRNA levels were maintained. The reduced R1 expression could be related to the reduction in the expression of p53R2, which was also seen in the heart and is discussed below.

4.3 RNR in resting cells

Recent studies of mammalian cells have shown that both R1 and p53R2 are expressed at a low, constitutive level, independent of the cell cycle (Håkansson *et al.*, 2006). While earlier studies have focused on the high levels of R1 in cycling cells, these studies suggest that R1 together with p53R2 form an active RNR enzyme in resting cells. In these cells RNR is assumed to provide dNTPs for DNA repair and mtDNA replication.

Findings in the present study demonstrated that in crucian carp the p53R2 genes are expressed in both heart and liver. In liver, p53R2 is transcribed at similar levels in both normoxia and anoxia, while in heart the transcription of p53R2 is reduced (~35%) upon anoxia exposure. It seems like

this reduction is coupled to the reduction of R1 expression in the same tissue, and this indicates that the level of p53R2 dependent RNR activity is lower in heart in anoxia than in normoxia. The reason for these reduced R1 and p53R2 levels may be that mitochondrial activity is low when glycolysis is the only ATP-producing process, and therefore there is a reduced need for RNR to provide dNTPs for mtDNA replication. Also, in the absence of oxygen there will be no oxidative stress in the cells, which is a major contributor to DNA damage. Reduced DNA damage would lead to reduced DNA repair activity, which consequently reduces the need to produce dNTPs. The leakage of reactive oxygen species from mitochondria during oxidative respiration is considered to be the most important cause of oxidative stress in aerobic organisms (Guidot *et al.*, 1993; Skulachev, 1999), and the production of dNTPs by R1 and p53R2 may therefore be directly related to both the number of mitochondria and the activity of these organelles. As the cardiac muscle cells can be expected to contain larger amounts of mitochondria compared to hepatocytes, it is reasonable that the effects of mitochondrial activity on expression of RNR proteins is more prominent in the heart than in the liver. In addition, the level of DNA repair activity is assumed to be both tissue-specific and to differ between proliferating and non-proliferating cells (Ono *et al.*, 2006; Simonatto *et al.*, 2007), and this may also contribute to the differences in R1/p53R2 expression observed in the heart and in the liver.

The indication of a higher expression of p53R2 subunits relative to the other quantified genes in liver than in heart may also suggest that there is a difference in the ratio of p53R2-dependent and R2-dependent activity between the two tissues. In the liver, the p53R2-dependent activity seems to contribute more to the total RNR activity than in the heart. The difference in the ratios of the R2/p53R2 subunits may reflect a difference in the ratio of proliferating and resting cells in these tissues, implying that the crucian carp heart has a higher relative amount of proliferating cells than the liver.

4.4   Is RNR activity possible in anoxic crucian carp?

Although the results of the real time RT-PCR experiments indicate that RNR proteins are present in crucian carp during anoxia, it is still uncertain if RNR enzymes remain active when oxygen is depleted. The formation of the radical is known to be oxygen dependent in class I RNR, and no radical formation has been observed at anaerobic conditions *in vitro* (Thelander *et al.*, 1983) or *in vivo* (Brischwein *et al.*, 1997). Once formed, the radical is stable during repeated catalytic cycles, but as the *in vivo* radical half-life has been observed to be about 10 min in mammals, the activity of RNR require the tyrosyl radical to be continuously regenerated (Chimploy *et al.*, 2000;

Thelander *et al.*, 1983). The activity of RNR is essential for cell division, and the finding of proliferating cells in crucian carp exposed to seven days of anoxia is therefore intriguing (Sollid *et al.*, 2005). If the crucian carp RNR is able to remain active at anaerobic conditions, one would expect the radical-generating parts of the enzyme, the R2/p53R2 subunits, to have different properties than in other class I enzymes.

The occurrence of several paralogs of each of the genes is in contrast to other vertebrates, where only one variant of each gene is found. This phenomenon is often observed when studying crucian carp genes, and is caused by polyploidy, i.e. the multiplication of entire sets of chromosomes beyond the normal set of two (Schultz, 1980). The immediate advantages of such events are not clear, but it is expected that once polyploidy is established there may be several possible benefits of having multiple copies of an allele (Leggatt and Iwama, 2003). One of these is the possibility of increasing the expression of key physiological proteins. Another is that genes are allowed to diverge in function. These advantages may well have contributed to the crucian carp adaptation to an extremely challenging environment. Regarding the RNR enzyme, one could imagine that the duplication of genes may have presented an opportunity to evolve proteins with divergent functions, possibly allowing one of the two copies to evolve to function during anaerobic conditions. However, based on the high pairwise sequence similarity (~95%) between all identified RNR paralogs, including the conservation of all known functional sites, the functionality should be preserved between the two variants of each protein.

The comparison of mammalian and crucian carp RNR amino acid sequences did not reveal any major differences between the functional sites of the proteins. Residues surrounding the iron center also seemed to be highly conserved. Moreover, the investigations of the crucian carp R2 and p53R2 radical center with EPR spectroscopy indicate that the chemical environment of the tyrosyl radical is highly similar to the mammalian counterparts. If the crucian carp RNR enzyme is functional in the absence of oxygen, it would presumably require either (A) that the radical is generated in a different, oxygen-independent manner, or (B) that the radical stability is extremely high compared to mammalian RNRs. As these properties would represent fundamental changes in what seems to be a well-conserved enzyme, one would expect this to be reflected in both the amino acid sequences and the EPR signals of the proteins constituting the enzyme. However, it could be that factors outside the RNR proteins contribute to stabilize the radical in crucian carp, and that also the low temperature at which the crucian carp experiences anoxia (8 °C in the present study) helps stabilizing the tyrosyl radical.

One may also consider whether the crucian carp can be supplied with dNTPs independently of RNR during anoxia. This could be made possible either by having a large dNTP pool in the cell, or by obtaining dNTP in a different oxygen-independent manner, such as through the salvage pathway. dNTP pools in the G_0 phase are normally very low. In the S phase and the G_2 phase, the size of the dNTP pools are at it largest. Nevertheless, the size of the smallest pool, usually dGTP, are generally considered to be sufficient for only a few minutes of DNA synthesis. Considering the fact that elevated dNTP pools have been associated with an increase in the rate of mutations (Elledge *et al.*, 1993), and that enabling cell proliferation throughout the anoxic period would require an extremely high pre-anoxic accumulation of dNTPs, corresponding to the whole genome, it seems unlikely that the RNR *de novo* activity can be substituted with large dNTP pool sizes. Another alternative could be that dNTPs are supplied through the salvage pathway, where material obtained from DNA degradation is reutilized by the activity of different kinases. This would, however, require a large supply of degraded DNA, either through nutrition or by degradation of cellular DNA. Food intake is expected to be minimal in crucian carp experiencing anoxia, and crucian carps experimentally exposed to anoxia are not fed, leaving degradation of DNA as the only available source of material for the salvage pathway. While this pathway has been considered to be able to supply dNTPs for DNA repair and mtDNA synthesis, *de novo* synthesis is considered essential when replicating genomic DNA in proliferating cells. Thus, it seems highly unlikely that the large amounts of dNTP needed for this task can be provided solely by degrading DNA.

4.5 Conclusions

Quantification of mRNA expression revealed that R1, R2 and p53R2 are present in both heart and liver tissues in normoxic and anoxic crucian carp.

Maintained levels of the cell cycle-specific R2 protein suggest that proliferating cells are present in both these tissues in anoxia, supporting previous observations of proliferating cells in anoxic crucian carp (Sollid *et al.*, 2005). In addition, the expression of proliferation-specific proteins in crucian carp heart suggest that the crucian carp share the relatively high proliferative rate of the zebrafish heart.

The p53R2 subunit probably provides dNTPs for DNA repair and for replication of mtDNA in resting cells in normoxic as well as anoxic crucian carp heart and liver, and it is possible that the reduced mitochondrial activity during anoxia is the cause of the reduction seen in the expression of both R1 and p53R2 in the anoxic heart.

As RNR sequences and EPR data revealed no major changes compared to mammalian RNR, it is still unclear if, and how, this enzyme can remain functionally active in anoxic crucian carp.

5 References

Ahuja, P., Sdek, P. and MacLellan, WR. (2007). Cardiac myocyte cell cycle control in development, disease, and regeneration. *Physiol Rev* **87**, 521-544.

Andersson, KK., Schmidt, PP., Katterle, B., Strand, KR., Palmer, AE., Lee, S., Solomon, EI., Gräslund, A. and Barra, A. (2003). Examples of high-frequency EPR studies in bioinorganic chemistry. *J Biol Inorg Chem* **8**, 235-247.

Arnér, ES. and Eriksson, S. (1995). Mammalian deoxyribonucleoside kinases. *Pharmacol Ther* **67**, 155-186.

Atkin, CL., Thelander, L., Reichard, P. and Lang, G. (1973). Iron and free radical in ribonucleotide reductase. Exchange of iron and Mössbauer spectroscopy of the protein B2 subunit of the Escherichia coli enzyme. *J Biol Chem* **248**, 7464-7472.

Atta, M., Andersson, KK., Ingemarson, R., Thelander, L. and Gräslund, A. (1994). EPR studies of mixed-valent [FeIIFeIII] clusters formed in the R2 subunit of ribonucleotide reductase from mouse or herpes simplex virus: mild chemical reduction of the diferric centers. *J Am Chem Soc* **116**, 6429-6430.

Björklund, S., Skog, S., Tribukait, B. and Thelander, L. (1990). S-phase-specific expression of mammalian ribonucleotide reductase R1 and R2 subunit mRNAs. *Biochemistry* **29**, 5452-5458.

Bleifuss, G., Kolberg, M., Pötsch, S., Hofbauer, W., Bittl, R., Lubitz, W., Gräslund, A., Lassmann, G. and Lendzian, F. (2001). Tryptophan and tyrosine radicals in ribonucleotide reductase: a comparative high-field EPR study at 94 GHz. *Biochemistry* **40**, 15362-15368.

Bollinger, JMJ., Edmondson, DE., Huynh, BH., Filley, J., Norton, JR. and Stubbe, J. (1991). Mechanism of assembly of the tyrosyl radical-dinuclear iron cluster cofactor of ribonucleotide reductase. *Science* **253**, 292-298.

Bourdon, A., Minai, L., Serre, V., Jais, J., Sarzi, E., Aubert, S., Chrétien, D., de Lonlay, P., Paquis-Flucklinger, V., Arakawa, H., Nakamura, Y., Munnich, A. and Rötig, A. (2007). Mutation of RRM2B, encoding p53-controlled ribonucleotide reductase (p53R2), causes severe mitochondrial DNA depletion. *Nat Genet* **39**, 776-780.

Brischwein, K., Engelcke, M., Riedinger, HJ. and Probst, H. (1997). Role of ribonucleotide reductase and deoxynucleotide pools in the oxygen-dependent control of DNA replication in Ehrlich ascites cells.. *Eur J Biochem* **244**, 286-293.

Brown, NC., Eliasson, R., Reichard, P. and Thelander, L. (1969). Spectrum and iron content of protein B2 from ribonucleoside diphosphate reductase. *Eur J Biochem* **9**, 512-518.

Burggren, WW. (1982). "Air gulping" improves blood oxygen transport during hypoxia in the goldfish, Carassius auratus.. *Physiol Zool* **55**, 327-334.

Byun, D., Chae, K., Ryu, B., Lee, M. and Chi, S. (2002). Expression and mutation analyses of P53R2, a newly identified p53 target for DNA repair in human gastric carcinoma. *Int J Cancer* **98**, 718-723.

Caras, IW., Levinson, BB., Fabry, M., Williams, SR. and Martin, DWJ. (1985). Cloned mouse ribonucleotide reductase subunit M1 cDNA reveals amino acid sequence homology with Escherichia coli and herpesvirus ribonucleotide reductases. *J Biol Chem* **260**, 7015-7022.

Chabes, A. and Thelander, L. (2000). Controlled protein degradation regulates ribonucleotide reductase activity in proliferating mammalian cells during the normal cell cycle and in response to DNA damage and replication blocks. *J Biol Chem* **275**, 17747-17753.

Chabes, AL., Pfleger, CM., Kirschner, MW. and Thelander, L. (2003). Mouse ribonucleotide reductase R2 protein: a new target for anaphase-promoting complex-Cdh1-mediated proteolysis. *Proc Natl Acad Sci U S A* **100**, 3925-3929.

Chenna, R., Sugawara, H., Koike, T., Lopez, R., Gibson, TJ., Higgins, DG. and Thompson, JD. (2003). Multiple sequence alignment with the Clustal series of programs. *Nucleic Acids Res* **31**, 3497-3500.

Chimploy, K., Tassotto, ML. and Mathews, CK. (2000). Ribonucleotide reductase, a possible agent in deoxyribonucleotide pool asymmetries induced by hypoxia.. *J Biol Chem* **275**, 39267-39271.

Covès, J., Laulhère, JP. and Fontecave, M. (1997). The role of exogenous iron in the activation of ribonucleotide reductase from Escherichia coli. *Jo Biol Inorg Chem* **2**, 418-426.

Cutler, P. (2003) Size-exclusion chromatography. In *Protein Purification Protocols*. Cutler, P. (ed). Humana Press, Totowa.

DeLano, WL. (2002). The PyMOL Molecular Graphics System, *published on World Wide Web http://www.pymol.org*.

Dong, Z., Liu, Y. and Zhang, J. (2005). Regulation of ribonucleotide reductase M2 expression by the upstream AUGs. *Nucleic Acids Res* **33**, 2715-2725.

Eklund, H., Uhlin, U., Färnegårdh, M., Logan, DT. and Nordlund, P. (2001). Structure and function of the radical enzyme ribonucleotide reductase. *Prog Biophys Mol Biol* **77**,

177-268.

Elledge, SJ., Zhou, Z., Allen, JB. and Navas, TA. (1993). DNA damage and cell cycle regulation of ribonucleotide reductase. *Bioessays* **15**, 333-339.

Ellefsen, S., Stensløkken, K-O., Sandvik, GK., Kristensen, TA. and Nilsson, GE. (2008). Improved normalization of real time RT PCR data using external RNA standard. *Anal Biochem* , doi: 10.1016/j.ab.2008.01.028.

Engström, Y., Eriksson, S., Jildevik, I., Skog, S., Thelander, L. and Tribukait, B. (1985). Cell cycle-dependent expression of mammalian ribonucleotide reductase. Differential regulation of the two subunits. *J Biol Chem* **260**, 9114-9116.

Eriksson, M., Uhlin, U., Ramaswamy, S., Ekberg, M., Regnström, K., Sjöberg, BM. and Eklund, H. (1997). Binding of allosteric effectors to ribonucleotide reductase protein R1: reduction of active-site cysteines promotes substrate binding. *Structure* **5**, 1077-1092.

Eriksson, S., Gräslund, A., Skog, S., Thelander, L. and Tribukait, B. (1984). Cell cycle-dependent regulation of mammalian ribonucleotide reductase. The S phase-correlated increase in subunit M2 is regulated by de novo protein synthesis. *J Biol Chem* **259**, 11695-11700.

Felsenstein, J. (1989). PHYLIP - Phylogeny Inference Package (Version 3.2). *Cladistics* **5**, 164-166.

Friedberg, EC. (2003). DNA damage and repair. *Nature* **421**, 436-440.

Gräslund, A. and Sahlin, M. (1996). Electron paramagnetic resonance and nuclear magnetic resonance studies of class I ribonucleotide reductase. *Annu Rev Biophys Biomol Struct* **25**, 259-286.

Guidot, DM., McCord, JM., Wrigth, RM. and Repine, JE. (1993). Absence of electron transport (Rho0 state) restores growth of a manganese-superoxide dismutase-deficient Saccharomyces cerevisiae in hyperoxia. Evidence for electron transport as a major source of superoxide generation in vivo. *J Biol Chem* **268**, 26699-26703.

Guittet, O., Hakansson, P., Voevodskaya, N., Fridd, S., Graslund, A., Arakawa, H., Nakamura, Y. and Thelander, L. (2001). Mammalian p53R2 protein forms an active ribonucleotide reductase in vitro with the R1 protein, which is expressed both in resting cells in response to DNA damage and in proliferating cells. *J Biol Chem* **276**, 40647-40651.

Gygi, SP., Rochon, Y., Franza, BR. and Aebersold, R. (1999). Correlation between protein and mRNA abundance in yeast. *Mol Cell Biol* **19**, 1720-1730.

Håkansson, P., Hofer, A. and Thelander, L. (2006). Regulation of mammalian ribonucleotide reduction and dNTP pools after DNA damage and in resting cells. *J Biol Chem* **281**, 7834-7841.

Herrick, J. and Sclavi, B. (2007). Ribonucleotide reductase and the regulation of DNA replication: an old story and an ancient heritage. *Mol Microbiol* **63**, 22-34.

Hollstein, M., Sidransky, D., Vogelstein, B. and Harris, CC. (1991). p53 mutations in human cancers. *Science* **253**, 49-53.

Holmgren, A. and Aslund, F. (1995). Glutaredoxin. *Methods Enzymol* **252**, 283-292.

Holmgren, A. and Björnstedt, M. (1995). Thioredoxin and thioredoxin reductase. *Methods Enzymol* **252**, 199-208.

Holopainen, IJ., Hyvärinen, H. and Piironen, J. (1986). Anaerobic wintering of crucian carp (Carassius carassius L.)--II. Metabolic products. *Comp Biochem Physiol A* **83**, 239-242.

Hyvärinen, H., Holopainen, IJ. and Piironen, J. (1985). Anaerobic wintering of crucian carp (Carassius carassius L.) 1. Annual dynamics of glycogen reserves in nature. *Comp Biochem Physiol A Physiol* **82**, 797-803.

Johansson, D., Nilsson, GE. and Døving, KB. (1997). Anoxic depression of light-evoked potentials in retina and optic tectum of crucian carp. *Neurosci Lett* **237**, 73-76.

Johnston, IA. and Bernard, LM. (1983). Utilization of the ethanol pathway in carp following exposure to anoxia. *J Exp Biol* **104**, 73-78.

Jordan, A. and Reichard, P. (1998). Ribonucleotide reductases. *Annu Rev Biochem* **67**, 71-98.

Kauppi, B., Nielsen, BB., Ramaswamy, S., Larsen, IK., Thelander, M., Thelander, L. and Eklund, H. (1996). The three-dimensional structure of mammalian ribonucleotide reductase protein R2 reveals a more-accessible iron-radical site than Escherichia coli R2. *J Mol Biol* **262**, 706-720.

Kimura, T., Takeda, S., Sagiya, Y., Gotoh, M., Nakamura, Y. and Arakawa, H. (2003). Impaired function of p53R2 in Rrm2b-null mice causes severe renal failure through attenuation of dNTP pools. *Nat Genet* **34**, 440-445.

Kolberg, M., Strand, KR., Graff, P. and Andersson, KK. (2004). Structure, function, and mechanism of ribonucleotide reductases. *Biochim Biophys Acta* **1699**, 1-34.

Leggatt, RA. and Iwama, GK. (2003). Occurence of polyploidy in the fishes. *Rev Fish Biol Fish* **13**, 237-246.

Lutz, PL. and Nilsson, GE. (1997). Contrasting strategies for anoxic brain survival--glycolysis up

or down. *J Exp Biol* **200**, 411-419.

Mann, GJ., Gräslund, A., Ochiai, E., Ingemarson, R. and Thelander, L. (1991). Purification and characterization of recombinant mouse and herpes simplex virus ribonucleotide reductase R2 subunit. *Biochemistry* **30**, 1939-1947.

Mann, GJ., Musgrove, EA., Fox, RM. and Thelander, L. (1988). Ribonucleotide reductase M1 subunit in cellular proliferation, quiescence, and differentiation. *Cancer Res* **48**, 5151-5156.

Mao, SS., Holler, TP., Yu, GX., Bollinger, JMJ., Booker, S., Johnston, MI. and Stubbe, J. (1992). A model for the role of multiple cysteine residues involved in ribonucleotide reduction: amazing and still confusing. *Biochemistry* **31**, 9733-9743.

Mathews, CK. and Ji, J. (1992). DNA precursor asymmetries, replication fidelity, and variable genome evolution. *Bioessays* **14**, 295-301.

Morrison, TB., Weis, JJ. and Wittwer, CT. (1998). Quantification of low-copy transcripts by continuous SYBR Green I monitoring during amplification. *Biotechniques* **24**, 954-962.

Nilsson, GE. (1990). Long-term anoxia in crucian carp: changes in the levels of amino acid and monoamine neurotransmitters in the brain, catecholamines in chromaffin tissue, and liver glycogen. *J Exp Biol* **150**, 295-320.

Nilsson, GE. (2007). Gill remodeling in fish--a new fashion or an ancient secret?. *J Exp Biol* **210**, 2403-2409.

Nilsson, GE., Rosen, PR. and Johansson, D. (1993). Anoxic depression of spontaneous locomotor activity in crucian carp quantified by a computerized imaging technique.. *J Exp Biol* **180**, 153-162.

Nordlund, P. and Eklund, H. (1993). Structure and function of the Escherichia coli ribonucleotide reductase protein R2. *J Mol Biol* **232**, 123-164.

Nordlund, P., Sjöberg, BM. and Eklund, H. (1990). Three-dimensional structure of the free radical protein of ribonucleotide reductase. *Nature* **345**, 593-598.

Nyholm, S., Mann, GJ., Johansson, AG., Bergeron, RJ., Gräslund, A. and Thelander, L. (1993). Role of ribonucleotide reductase in inhibition of mammalian cell growth by potent iron chelators. *J Biol Chem* **268**, 26200-26205.

Ochiai, E., Mann, GJ., Gräslund, A. and Thelander, L. (1990). Tyrosyl free radical formation in the small subunit of mouse ribonucleotide reductase. *J Biol Chem* **265**, 15758-15761.

Ono, T., Ikehata, H., Uehara, Y. and Komura, J. (2006). The maintenance of genome integrity is tissue-specific. *Genes and Environment* **28**, 16-22.

Palmer, G. (2000) Electron paramagnetic resonance of metalloproteins. In *Physical methods in bioinorganic chemistry - spectroscopy and magnetism.* Que, L. (ed). University Science Books.

Persson, AL., Eriksson, M., Katterle, B., Pötsch, S., Sahlin, M. and Sjöberg, BM. (1997). A new mechanism-based radical intermediate in a mutant R1 protein affecting the catalytically essential Glu441 in Escherichia coli ribonucleotide reductase. *J Biol Chem* **272**, 31533-31541.

Pfaffl, MW. (2001). A new mathematical model for relative quantification in real-time RT-PCR. *Nucleic Acids Res* **29**, e45.

Pontarin, G., Ferraro, P., Håkansson, P., Thelander, L., Reichard, P. and Bianchi, V. (2007). p53R2-dependent ribonucleotide reduction provides deoxyribonucleotides in quiescent human fibroblasts in the absence of induced DNA damage. *J Biol Chem* **282**, 16820-16828.

Poss, KD., Wilson, LG. and Keating, MT. (2002). Heart regeneration in zebrafish. *Science* **298**, 2188-2190.

Powell, DR., Desai, U., Sparks, MJ., Hansen, G., Gay, J., Schrick, J., Shi, Z., Hicks, J. and Vogel, P. (2005). Rapid development of glomerular injury and renal failure in mice lacking p53R2. *Pediatr Nephrol* **20**, 432-440.

Rasmussen R (2001) Quantification on the LightCycler. In *Rapid Cycle Real-time PCR, Methods and Applications.* Meuer, S, Wittwer, C, Nakagawara, K (ed). Springer press, Heidelberg.

Reichard, P. (1988). Interactions between deoxyribonucleotide and DNA synthesis. *Annu Rev Biochem* **57**, 349-374.

Reichard, P. (1993). From RNA to DNA, why so many ribonucleotide reductases?. *Science* **260**, 1773-1777.

Reichard, P. and Ehrenberg, A. (1983). Ribonucleotide reductase--a radical enzyme. *Science* **221**, 514-519.

Ririe, KM., Rasmussen, RP. and Wittwer, CT. (1997). Product differentiation by analysis of DNA melting curves during the polymerase chain reaction. *Anal Biochem* **245**, 154-160.

Røhr, ÅK. (2001) Electron paramagnetic resonance studies of the mixed valence diiron-oxygen cluster in the mouse ribonucleotide reductase R2 protein. *Master thesis,* University of Oslo.

Roy, SW., Fedorov, A. and Gilbert, W. (2003). Large-scale comparison of intron positions in mammalian genes shows intron loss but no gain. *Proc Natl Acad Sci U S A* **100**, 7158-7162.

Rozen, S. and Skaletsky, H. (2000) Primer3 on the WWW for general users and for biologist

programmers. In *Bioinformatics: methods and protocols*. Misener, S. and Krawetz, SA. (ed). Humana Press, Totowa.

Sahlin, M., Sjöberg, BM., Backes, G., Loehr, T. and Sanders-Loehr, J. (1990). Activation of the iron-containing B2 protein of ribonucleotide reductase by hydrogen peroxide. *Biochem Biophys Res Commun* **167**, 813-818.

Schultz, J. (1980) Role of polyplidy in the evolution of fishes. In *Polyploidy: Biological Relevance*. Lewis, WH. (ed). Plenum Press, New York.

Scotto-Lavino, E., Du, G. and Frohman, MA. (2006a). 3' end cDNA amplification using classic RACE. *Nat Protoc* **1**, 2742-2745.

Scotto-Lavino, E., Du, G. and Frohman, MA. (2006b). 5' end cDNA amplification using classic RACE. *Nat Protoc* **1**, 2555-2562.

Selkirk, C. (2003) Ion-exchange chromatography. In *Protein Purification Protocols*. Cutler, P. (ed). Humana Press, Totowa.

Shoubridge, EA. and Hochachka, PW. (1980). Ethanol: novel end product of vertebrate anaerobic metabolism. *Science* **209**, 308-309.

Simonatto, M., Latella, L. and Puri, PL. (2007). DNA damage and cellular differentiation: more questions than responses. *J Cell Physiol* **213**, 642-648.

Sjöberg, BM., Karlsson, M. and Jörnvall, H. (1987). Half-site reactivity of the tyrosyl radical of ribonucleotide reductase from Escherichia coli. *J Biol Chem* **262**, 9736-9743.

Skulachev, VP. (1999). Mitochondrial physiology and pathology: concepts of programmed death of organelles, cells and organisms. *Mol Aspects Med* **20**, 139-184.

Smith, RW., Houlihan, DF., Nilsson, GE. and Alexandre, J. (1999). Tissue-specific changes in RNA synthesis in vivo during anoxia in crucian carp. *Am J Physiol* **277**, R690-7.

Smith, RW., Houlihan, DF., Nilsson, GE. and Brechin, JG. (1996). Tissue-specific changes in protein synthesis rates in vivo during anoxia in crucian carp. *Am J Physiol* **271**, R897-904.

Sollid, J. and Nilsson, GE. (2006). Plasticity of respiratory structures--adaptive remodeling of fish gills induced by ambient oxygen and temperature. *Respir Physiol Neurobiol* **154**, 241-251.

Sollid, J., De Angelis, P., Gundersen, K. and Nilsson, GE. (2003). Hypoxia induces adaptive and reversible gross morphological changes in crucian carp gills.. *J Exp Biol* **206**, 3667-3673.

Sollid, J., Kjernsli, A., De Angelis, PM., Røhr, AK. and Nilsson, GE. (2005). Cell proliferation and gill morphology in anoxic crucian carp. *Am J Physiol Regul Integr Comp Physiol* **289**, R1196-201.

Stecyk, JAW., Stensløkken, K., Farrell, AP. and Nilsson, GE. (2004). Maintained cardiac pumping in anoxic crucian carp. *Science* **306**, 77.

Strand, KR., Karlsen, S., Kolberg, M., Røhr, AK., Görbitz, CH. and Andersson, KK. (2004). Crystal structural studies of changes in the native dinuclear iron center of ribonucleotide reductase protein R2 from mouse. *J Biol Chem* **279**, 46794-46801.

Suzue, T., Wu, GB. and Furukawa, T. (1987). High susceptibility to hypoxia of afferent synaptic transmission in the goldfish sacculus. *J Neurophysiol* **58**, 1066-1079.

Svistunenko, DA. and Cooper, CE. (2004). A new method of identifying the site of tyrosyl radicals in proteins. *Biophys J* **87**, 582-595.

Symons, M. (1978) *Chemical and biochemical aspects of electron-spin resonance spectroscopy.* Van Nostrand Reinhold Company, New York.

Tanaka, H., Arakawa, H., Yamaguchi, T., Shiraishi, K., Fukuda, S., Matsui, K., Takei, Y. and Nakamura, Y. (2000). A ribonucleotide reductase gene involved in a p53-dependent cell-cycle checkpoint for DNA damage. *Nature* **404**, 42-49.

Thelander, L. and Berg, P. (1986). Isolation and characterization of expressible cDNA clones encoding the M1 and M2 subunits of mouse ribonucleotide reductase. *Mol Cell Biol* **6**, 3433-3442.

Thelander, L. and Reichard, P. (1979). Reduction of ribonucleotides. *Annu Rev Biochem* **48**, 133-158.

Thelander, L., Gräslund, A. and Thelander, M. (1983). Continual presence of oxygen and iron required for mammalian ribonucleotide reduction: possible regulation mechanism. *Biochem Biophys Res Commun* **110**, 859-865.

Tichopad, A., Didier, A. and Pfaffl, MW. (2004). Inhibition of real-time RT-PCR quantification due to tissue-specific contaminants. *Mol Cell Probes* **18**, 45-50.

Tomter, AB. (2006) Spectroscopic studies of the diiron oxygen cluster and tyrosyl radical in the p53 induced human ribonucleotide reductase p53R2. *Master thesis,* University of Oslo.

Uhlin, U. and Eklund, H. (1994). Structure of ribonucleotide reductase protein R1. *Nature* **370**, 533-539.

van Waversweld, J., Addink, ADF. and van den Thillart, G. (1989). Simultaneous Direct and Indirect Calorimetry on Normoxic and Anoxic Goldfish. *J Exp Biol* **142**, 325-335.

Welch, BL. (1947). The generalization of "student's" problem when several different population variances are involved. *Biometrika* **34**, 28-35.

Welin, M., Ogg, D., Arrowsmith, C., Berglund, H., Busam, R., Collins, R., Edwards, A., Ehn, M., Flodin, S., Flores, A., Graslund, S., Hammarstrom, M., Hallberg, BM., Holmberg Schiavone, L., Hogbom, M., Kotenyova, T., Magnusdottir, A., Moche, M., Nilsson-Ehle, P., Nyman, T., Persson, C., Sagemark, J., Sundstrom, M., Stenmark, P., Uppenberg, J., Thorsell, AG., Van Den Berg, S., Wallden, K., Weigelt, J. and Nordlund, P.. (2007) Crystal Structure of Human Ribonucleotide Reductase Subunit R2, *DOI 10.2210/pdb2uw2/pdb*.

Wilson, IG. (1997). Inhibition and facilitation of nucleic acid amplification. *Appl Environ Microbiol* **63**, 3741-3751.

6 Appendices

6.1 Appendix I: Abbreviations

5'-UTR	5'-untranslated region
ADP	adenosine diphosphate
BrdU	5'-bromo-2'-deoxyuridine
cDNA	complementary DNA
CDP	cytidine 5'-diphosphate
dADP	deoxyadenosine 5'-diphosphate
dATP	deoxyadenosine 5'-triphosphate
dCDP	deoxycytidine 5'-diphosphate
dCMP	deoxycytidine 5'-monophosphate
dCTP	deoxycytidine 5'-triphosphate
dGDP	deoxyguanosine 5'-diphosphate
dGTP	deoxyguanosine 5'-triphosphate
dNDP	deoxynucleoside 5'-diphosphate
dNTP	deoxynucleoside 5'-triphosphate
dTTP	deoxythymidine 5'-triphosphate
dUDP	deoxyuridine 5'-diphosphate
EPR	electron paramagnetic resonance
GDP	guanosine 5'-diphosphate
GSP	gene specific primer
ILCM	inter lamellar cell material
IPTG	isopropyl β-D-1-thiogalactopyranoside
mRNA	messenger ribonucleic acid
mtDNA	mitochondrial DNA
NADPH	nicotinamide adenine dinucleotide phosphate (reduced form)
NDP	nucleoside 5'-diphosphate
p53R2	p53 inducible ribonucleotide reductase subunit
PCNA	proliferating cell nuclear agent
R1	ribonucleotide reductase subunit 1
R2	ribonucleotide reductase subunit 2
RACE	rapid amplification of cDNA ends
RNR	ribonucleotide reductase
RT-PCR	reverse transcription polymerase chain reaction
SDS-PAGE	sodium dodecyl sulphate polyacrylamide gel electrophoresis
UDP	uridine 5'-diphosphate
UTR	untranslated region
X-gal	5-bromo-4-chloro-3-indolyl- beta-D-galactopyranoside

6.2 Appendix II: Reagents, equipment and software

Reagents (product, catalog number and manufacturer)

Advtantage 2 polymerase mix, Clontech Laboratories Inc., Mountain View, USA

Agarose, SeaKem, 50004, Cambrex

Ampicillin (D[-]-α-Aminobenzylpenicillin), A-9518, Sigma

BL21-Gold(DE3) *E. coli* cells, 230132, Stratagene

dNTP-mix, 10297-018, Invitrogen

Dithiothreitol, Y00147, Invitrogen

Dynabeads mRNA Direct Kit, 610.01 Invitrogen

Etidium bromide, 443922U, BHD-Electron

UltraPure Glycerol, 15514-011, Invitrogen

Generacer Kit, L-1500, Invitrogen

*Hind*III restriction enzyme, ER0501, Fermentas

HiTrap desalting columns, 17-1408-01, GE Healthcare

HiTrap Q HP columns, 11-0013-03, GE Healthcare

IPTG (isopropyl-β-D-thio-galactoside), 21727117, Promega

LightCycler FastStart DNA Master^{PLUS} SYBR Green I, 04707516001, Roche Diagnostics

Low Molecular Weight Calibration Kit for SDS Electrophoresis, 17-0446-01, GE Healthcare

*Nde*I restriction enzyme, ER0581, Fermentas

pET-22b Expression Vector System, Novagen

pGEM-T Easy Vector Systems, A1360, Promega

Phast Gel System, GE Healthcare

Phusion High Fidelity DNA Polymerase, F-530, Finnzymes

GeneJET PCR Cloning Kit, K1221/2, Fermentas

Platinum Taq Polymerase, 10966, Invitrogen

*Sal*I restriction enzyme, ER0642, Fermentas

SMART RACE cDNA Amplification Kit, 634914, Clontech

SOC medium, 15544-034, Invitrogen

Superdex 200 HR 10/300 column, GE Healthcare

Superscript III Reverse Transcriptase, 18080-(044), Invitrogen

T4 DNA Ligase, M1801, Promega

TRIzol Reagent, 15596-018, Invitrogen

TURBO DNA-free Kit, Cat #1907, Ambion

Wizard Plus SV Minipreps DNA Purification System, TB225, Promega

Wizard SV Gel and PCR Clean-Up System, A9281/A9282, Promega

X-Gal, V3941, Promega

Equipment (product, catalog number/model and manufacturer)

Äkta Purifier System, GE Healthcare

Agilent 2100 Bioanalyzer, G2938B, Agilent

Amicon ultra centrifugal filter devices, UFC903008, Millipore

Avanti J-25 centrifuge, Beckman

BioDoc-It System (UV light gel picturing machine), UVP

Elexys 560 spectrometer with ER4116DM dual mode resonator cavity, Bruker

Eppendorf centrifuge, 5417R, Eppendorf

Finnpipettes, 0.5-10 µl, U23386; 2-20 µl, T27033; 20-200 µl, T27388; 100-1000 µl, T28301,
      Thermo Labsystems

ESR900 Liquid Helium control system, Oxford Instruments

Homogenizer, Duall 22, Kontes glass

Homogenizer, Ultra-Turrax T8, IKA

LightCycler 480 Instrument, 03531414201, Roche

Mastercycler gradient, 5331, Eppendorf

NanoDrop, Model ND-1000, NanoDrop Technologies

N2-gas, AGA

X-press hydraulic press, AB BIOX

Software (freeware is listed with websites)

Äkta UNICORN software, version 3.1 , GE Healthcare

BioEdit, version 7.0.9 (http://www.mbio.ncsu.edu/BioEdit/bioedit.html)

BoxShade, version 3.2 (http://www.ch.embnet.org/software/BOX_form.html)

Chemtool, version 1.6.10 (http://ruby.chemie.uni-freiburg.de/~martin/chemtool/)

ClustalX and ClustalW, version 2.0 (http://bips.u-strasbg.fr/fr/Documentation/ClustalX/)

LightCycler® Software, version 4.0, Roche Applied Science

MiniTab Statistical Software, version 15, Minitab Inc.

NanoDrop, version 3.0.1, Coleman Technologies Inc.

Netblast, version 2.2.17 (http://www.ncbi.nlm.nih.gov/blast/download.shtml)

Phylip, version 3.67 (http://evolution.genetics.washington.edu/phylip.html)

Primer3 primer design program, version 0.4.0 (http://frodo.wi.mit.edu/)

PyMol molecular graphics and modelling package, version 1.0 (http://pymol.sourceforge.net/)

SeaView (http://pbil.univ-lyon1.fr/software/seaview.html)

WinEPR, Bruker BioSpin

6.3   Appendix III: GenBank accession numbers for RNR genes

Gene	Organism	GenBank accession number
R1	Chicken (*Gallus gallus*)	NP_001026008.1
	African clawed frog (*Xenopus laevis*)	NP_001084312.1
	Human (*Homo sapiens*)	NP_001024.1
	Mouse (*Mus musculus*)	NP_033129.2
	Pufferfish (*Tetraodon nigroviridis*)	CAG02916.1
	Zebrafish (*Danio rerio*)	NP_571530.1
R2	Chicken (*Gallus gallus*)	XP_419948.2
	Crucian carp (*Carassius carassius*)	AAY82584.1[a]
	African clawed frog (*Xenopus laevis*)	NP_001080772.1
	Human (*Homo sapiens*)	NP_001025.1
	Mouse (*Mus musculus*)	NP_033130.1
	Zebrafish (*Danio rerio*)	NP_571525.1
p53R2 (R2 B)	Chicken (*Gallus gallus*)	XP_418364.2
	Human (*Homo sapiens*)	NP_056528.2
	Mouse (*Mus musculus*)	NP_955770.1
	Pufferfish (*Tetraodon nigroviridis*)	CAF96041.1
	Zebrafish (*Danio rerio*)	NP_001007164.1

[a]Partial sequence.

6.4 Appendix IV: Crucian carp RNR cDNA sequences

The following crucian carp RNR sequences were obtained by cloning. Predicted start and stop codons are shown in inverted colors. Real time RT-PCR products are denoted in bold.

R1.1 cDNA

```
   1   GTATTTCATAGACATCAGTCTGCAGAAGCAACTGAGGGGTCGGTTAACAGAATAGCACTT     60
  61   TATCCACAAATACTCCTAATTCGTTTTTTTCCTCTGTTTTCTTTAGCAGAGACGTCAATC    120
 121   ATGCACGTGATCAAGAGAGATGGTCGCCAGGAGCGTGTTATGTTCGACAAAATCACATCA    180
 181   CGCATCCAGAAACTTTGCTATGGACTCAATGCCGAGTTTGTTGATCCTACTCATATCACC    240
 241   ATGAAGGTGATTCAGGGCCTTTACAGCGGTGTTACCACAGTAGAGCTGGACACCCTGGCT    300
 301   GCTGAGATCTCTGCCACCCTCACCACCAAACACCTGACTATGCCATCCTGGCGGCCCGC    360
 361   ATCGCTGTGTCCAACCTGCACAAAGAAACCAAGAAGGTCTTCAGTGAGGCTATGGAGGAC    420
 421   CTCTACAACTATGTGAATCCCCTGAATGACCGCCACTCACCTATGGTTTCAAAGGAAACC    480
 481   CTCGACATTGTTTTGGCCAACAAAGATAGACTCAACTCGGCCATCATTTTTGACAGAGAT    540
 541   TTCTCTTACAACTTCTTTGGCTTCAAGACATTGGAGCGCTCGTATCTGCTAAAGATCAAT    600
 601   GGGAAAGTCGCCGAGCGGCCACAACACATGCTGATGAGGGTGTCCGTGGGAATCCATAAA    660
 661   GAGGACATTGCGGCAGCTATAGAAACCTACAATCTGCTCTCTGAGAAGTGGTTCACTCAC    720
 721   GCTTCTCCTACACTGTTCAACGCCGGCACCAACCGGCCACAGCTCTCCAGTTGCTTCCTG    780
 781   CTTGCTATGAAAGATGACAGTATTGATGGGATCTATGACACCCTGAAGCAGTGCGCCCTC    840
 841   ATTTCTAAGTCGGCCGGAGGTATTGGGGTGGCAGTGAGCTGCATTAGAGCTACTGGAAGC    900
 901   TACATTGCAGGGACTAATGGGAACTCAAATGGCCTGGTTCCTATGCTCCGTGTCTACAAC    960
 961   AACACAGCACGTTATGTGGACCAAGGAGGAAATAAGAGACCAGGAGCTTTTGCTATGTAC   1020
1021   CTGGAGCCCTGGCATTTTGACATCTTTGACTTCCTAGAGCTTAAAAAGAATACTGGTAAA   1080
1081   GAGGAGCAGAGAGCCAGAGATCTGTTTTATGCCCTCTGGATCCCTGATCTCTTCATGAAG   1140
1141   CGTGTGGAGACCAATGGGGATTGGTGTCTGATGTGCCCTAATGACTGTCCCGGGCTGGAT   1200
1201   GAGTGCTGGGGAGAGGAATTTGAGAATCTCTACACAAAATATGAGAAGGAGGGCAAAGCT   1260
1261   AAGCGTGTGGTGAAGGCTCAGCAGCTGTGGCATGCCATCATTGAGTCGCAGACAGAGACC   1320
1321   GGAACACCCTACATGCTCTATAAGGATGCCTGTAACCGCAAGAGCAACCAGCAGAACCTG   1380
1381   GGCACCATCAAATGCAGTAATCTGTGCACCGAGATTGTAGAGTACACCAGTAAGGATGAG   1440
1441   GTGGCTGTTTGCAACTTAGCATCCGTTGCACTTAACATGTACGTCACCCCAGAGCGAACT   1500
1501   TTTGACTTCCAGAAGTTGGCCTCTGTTACAAAAGTCATTGTGAAGAACCTGAACAAAATC   1560
1561   ATTGATATCAACTACTATCCTGTGCAAGAGGCAGAGAATTCCAACAAGCGTCACAGGCCC   1620
1621   ATCGGTATCGGCGTTCAGGGTCTGGCTGATGCCTTCATCCTCATGCGCTTCCCATTTGAG   1680
1681   AGCGCAGAGGCTCAACTCCTCAACACACAGATCTTTGAGACAATCTACTACGCTGCGCTG   1740
1741   GAGTCCAGCTGTGAGCTGGCTGCGGAATTTGGGCCGTATGAAACGTACGCTGGGTCTCCT   1800
1801   GTGAGCAAGGGCATCCTGCAGTATGATATGTGGGATAAGACCCCTACAGACCTGTGGGAC   1860
1861   TGGGAGGCACTCAAGGAGAAGATTGCCAAGCATGGAGTGCGTAACAGTCTGCTGCTGGCT   1920
1921   CCTATGCCCACTGCCTCCACTGCTCAGATCCTGGGAAACAACGAGTCAATCGAGCCATAC   1980
1981   ACTAGCAACATCTACACACGCAGAGTTCTGTCTGGAGAGTTTCAGATTGTGAACCCACAT   2040
2041   CTTCTCAAAGACCTCACGGAACGAGGACTTTGGAATGAAGAAATGAAAACCAGCTAATT   2100
2101   GCTCAGAACGGATCCATCCAAGGCATCCCCACAATACCAGATGACCTGAAAGAGCTGTAC   2160
2161   AAGACCGTGTGGGAGATCTCTCAAAAGACCATCTTAAAGATGGCTGCAGACAGAGGAGCC   2220
2221   TTCATTGACCAGAGCCAGTCTCTCAACATCCACATCGCTGAACCCAACTATGGCAAACTG   2280
2281   ACCAGCATGCACTTCTATGGCTGGAAGCAGGGTCTTAAAACAGGAATGTACTACCTGAGA   2340
2341   ACTAAACCAGCTGCCAACCCCATCCAGTTCACTCTCAACAAAGAAAAACTGAAGGAGACG   2400
2401   CAGAAAAGTGCAAGCAACGAGGAGGAAATCAAAGAACTCAACATGGCTGCTATGGTGTGT   2460
2461   TCACTGGAGAACCGTGACGAGTGTCTGATGTGTGGTTCATGAACTCAGCTCCTGTTGACA   2520
2521   AGGACCATTAGGATGGTTGCCAATTTGCATTAGTTTTTGAAAGGACACGTGCGATTTGTT   2580
2581   TAGCTTGGGTGAAATAAAGTACAGACTAACTAAAAAAAAAAAAAAAAAA             2629
```

R1.2 cDNA

```
   1   TGGCGCGCGCTAGTACAACAACAGCTGAGAGAGCCGCGAGCAGAACAGCACTTTTCCAAA    60
  61   AATAACACCCGATTATTATTATTTGTCCTCTCTACCGAGACTTTAATCATGCACGTGATC   120
 121   AAGAGAGATGGGCACCAGGAGCGTGTTATGTTCGACAAAATCACATCACGTATCCAGAAA   180
 181   CTTTGTTATGGACTCAACGCTGAGTTTGTTGATCCTACTCAGATCACCATGAAGGTGATT   240
 241   CAGGGCCTTTACAGCGGTGTCACCACAGTAGAGCTGGACACCCTGGCTGCTGAGATCACT   300
 301   GCCACCCTCACCACCAAACACCCTGACTATGCCATCCTGGCGGCCCGCATCGCTGTGTCC   360
 361   AACCTGCACAAAGAAACCAAGAAGGTCTTCAGTGAGGTTATGGAGGACCTCTACAACTAT   420
 421   GTGAATCCCCTGAACGGCCACCACTCGCCTATGATTTCCAAGGAAACCCTCGACATTGTT   480
 481   TTAGCCAACAAAGATCGGCTCAACTCTGCCATCATTTTTGACAGAGATTTCTCCTACAAC   540
 541   TTCTTTGGCTTCAAGACATTGGAGCGCTCATATCTGCTGAAGATCAATGGAAAGGTTGCT   600
 601   GAGCGGCCACAACACATGCTGATGAGAGTGTCTGTGGGAATCCATAAGGAGGACATTGCG   660
 661   GCAGCTATAGAAACCTACAACCTGCTGTCTGAGAAGTGGTTCACTCATGCTTCTCCTACA   720
 721   CTCTTCAATGCCGGCACCAACCGGCCACAGCTCTCCAGTTGCTTCCTGCTTGCTATGAAG   780
 781   GATGACAGTATTGAGGGGATCTATGACACCTTGAAGCAGTGCGCCCTCATTTCTAAGTCT   840
 841   GCGGGAGGTATCGGGGTGGCAGTGAGCTGCATTAGAGCCACTGGCAGCTACATCGCAGGG   900
 901   ACAAATGGCAACTCAAATGGCCTGGTTCCTATGCTCCGTGTCTACAACAACACCGCACGC   960
 961   TATGTGGATCAAGGAGGAAATAAGAGACCTGGAGCTTTTGCCATGTACCTGGAGCCCTGG  1020
1021   CATTTTGACATTTTCGACTTCCTAGAGCTTAAAAAGAACACCGGTAAAGAGGAACAGAGA  1080
1081   GCTAGAGATCTGTTTTACGCCCTCTGGATCCCCGATCTCTTCATGAAGCGAGTGGAGACC  1140
1141   AATGCGGACTGGTCTCTGATGTGCCCCAGTGACTGTCCCGGGCTGGATGAGTGCTG**GGGA**  1200
1201   **GAGGAATTTGAGAAGCTCTACATGAAATATGAGCAGGAGGGAAGAGCTAAGCGTGTGGTG**  1260
1261   **AAGGCTCAGCAGCTGTGGTATGCCATCATTGAGTCTCAGACAGAGACCGGCACACCCTAC**  1320
1321   **ATGCTCTACAAGGACGCCTGCAACCGCAAAAGCAACCAGCAGAACCTGGGCACCATTAAA**  1380
1381   **TGCAGTAACCTGTGCACAGAAATTGTAGAGTACACCAGTAAGG**ATGAGGTTGCAGTTTGC  1440
1441   AACCTGGCGTCCATCGCACTTAACATGTACGTCACCCCAGAACGAACTTTTGACTTCCAG  1500
1501   AAGCTGGCATCTGTTACGAAAGTCATTGTGAAAAACCTAAACAAAATCATCGATGTCAAC  1560
1561   TACTACCCAGTGCGAGAGGCAGAAAATTCCAACAAGCGTCACAGGCCCATCGGTATCGGC  1620
1621   GTTCAGGGTCTGGCTGATGCCTTTATTCTCATGCGTTTCCCCTTTGAGAGCGCAGAGGCT  1680
1681   CAGCTCCTCAACACACAGATCTTTGAGACCATCTACTACGCTGCGCTGGAGTCCAGCTGT  1740
1741   GAGCTGGCTGCGGAATGTGGGCCGTATGAAACATATGCTGGCTCTCCTGTGAGCAAGGGC  1800
1801   ATCCTGCAGTATGATATGTGGGAGAAGACACCTACAGACCTGTGGGACTGGGCCGCACTC  1860
1861   AAGGAGAAGATCACAAAGCATGGAGTGCGTAACAGTCTGCTGCTGGCTCCCATGCCCACT  1920
1921   GCCTCCACTGCTCAGATCCTGGGCAACAACGAGTCAATCGAGCCGTATACTAGCAACATC  1980
1981   TACACACGCAGAGTTCTGTCTGGAGAGTTTCAGATTGTGAACCCACATCTTCTCAAAGAC  2040
2041   CTCACAGAACGAGGACTTTGGAACGAAGAAATGAAAAACCAGTTAATCGCTCAGAACGGA  2100
2101   TCCATTCAGGCTATTCCCACAATACCAGATGACCTGAAGGAGCTGTATAAGACTGTGTGG  2160
2161   GAGATCTCTCAAAAGACCATCTTAAAGATGGCTGCGGACAGAGGAGCCTTCATTGACCAG  2220
2221   AGCCAGTCCCTCAACATCCACATTGCTGAACCCAACTATGGCAAACTGACCAGCATGCAC  2280
2281   TTCTATGGCTGGAAGCAGGGTCTTAAAACAGGAATGTACTACCTGAGAACTAAACCAGCC  2340
2341   GCCAACCCCATCCAGTTCACTCTCGACAAAGAAAACTGAAGGAGACGCAGGAAAGTACA  2400
2401   AGCAACGAGGAGGAAACCAAAGAACGCAACAAAGCAGCTATGGTGTGTTCATTGGAGAAC  2460
2461   CGTGATGAGTGTCTGATGTGCGGTTCA**TGA**ATTGATCCTCCTGTGACAGGACCATTAGGA  2520
2521   TGGCTAACGATATGCATCTTATACAGTATTATATCTTTTTTAAATGGGCTTAGAAGAATA  2580
2581   TCATTTACATTTTCTGTAWACAATACCAGAAGATTCATAAAAGTCTACTTGGATCAAAAA  2640
2641   AAAAAAAAAA                                                    2650
```

R2.1 cDNA

```
   1  GGTTTTCTTTCTTTCAGCTGGGCTTCACCTGTTAGATCTTTAAGCTTACGCTTTCCATTT   60
  61  TATTTATTTTGCTGACTTTGTTTTAGAAGTTGTTCATCTTTTTAACTTATCCTCATTTTC   120
 121  TGTTTGACCTAACACTTTAAGCTTTAACAAATGCAGTCAACTCGCTCTCCACTGAAAACTA   180
 181  AGAACGAAAACACAATTTCTGCCAAAATCAACAACATGTCCTTGGTGGACAAAGAAAACA   240
 241  CGCCGCCCAGCCTGAGCTCCAGCAGGATCCTGGCGTCCAAAACGGCGCGCAAAATCTTTG   300
 301  ATTCAGAGGAGCAGACAAAAGCTAAGAAAGGAGCTGTGGAGGAGGAGCCCCTTCTGAAGG   360
 361  AGAACCCCCACCGCTTTGTCATTTTCCCAATTCAGTACCATGACATCTGGCAGATGTACA   420
 421  AGAAGGCAGAGGCCTCTTTCTGGACTGCAGAGGAGGTTGACCTGTCCAAAGATCTTCAGC   480
 481  ACTGGGACTCCCTGAAAGACGAGGAGAGATACTTCATCTCTCATGTTTTGGCTTTTTTCG   540
 541  CTGCGAGTGATGGCATCGTCAATGAGAACTTGGTGGAGCGATTTACTCAGGAAGTCCAAG   600
 601  TGACTGAAGCCCGTTGCTTCTACGGTTTCCAGATTGCCATGGAAAACATCCACTCTGAAA   660
 661  TGTACAGTCTGTTGATTGACACCTACATAAAAGATCCCAAAGAGAGAGAATTTCTCTTCA   720
 721  ATGCCATTGAGACCATGCCTTGCGTAAAGAAGAAGGCCGACTGGGCGCTCAACTGGATTG   780
 781  GTGACAAAAATGCACAATACGGGGAGAGAGTGGTGGCTTTCGCTGCTGTGGAAGGAATCT   840
 841  TCTTTTCTGGGTCTTTTGCTTCTATTTTCTGGCTAAAGAAGAGAGGACTCATGCCGGGAC   900
 901  TCACCTTCTCCAATGAACTTATCAGCAGAGATGAGGGTCTACACTGTGACTTTGCCTGCC   960
 961  TCATGTTCAAGCACTTGGTCAACAAACCTTCGGAGGCAACCGTAAAGAAAATCATCATGA   1020
1021  ATGCAGTTGAGATTGAACAGGAATTCCTGACTGATGCTCTGCCAGTAAAGCTTATTGGCA   1080
1081  TGAATTGTGACCTGATGAAGCAATACATTGAGTTTGTGGCTGATAGACTTCTGCTGGAGC   1140
1141  TGGGATTTGACAAGGTCTATAAAGTGGAAAATCCTTTTGACTTCATGGAGAACATTTCCT   1200
1201  TGGAGGGGAAGACCAACTTCTTTGAGAAGCGAGTCGGCGAGTACCAGCGGATGGGAGTCA   1260
1261  TGTCCGGACCCACCGATAACACTTTCAGGCTGGATGCTGATTTTTAGAGTTTTCTTACGA   1320
1321  GTGCATGAATGGAAGCAAACTATGAACTGTTTGGACTCTGAGGAGATTCGACCTCACTTA   1380
1381  TTTCTACAGTTTGTTTAATTCATTTTTTTTTTTTTTTTTTTTTTT                  1425
```

R2.2 cDNA

```
   1  GTTTTCTTTCCTTCAGCTGGACTGTGGATTTTCAATGTTTTACTTTTAATTTTATTTATT   60
  61  TGTAGCTTACTTTGTTTTAGAAGTTTTTTTTTTATTATCCTTATTTTCTGTTTTATCTAA   120
 121  CACTATAAGCTTTGCAATGTCGTCAACTCGCTCTCCACTGAAAACCAAGAATGAAAACGC   180
 181  CGTTTTTGCAAAAATGACTAACATGTCCTTGGTGGACAAAGAAAACACGCCACCCAGTCT   240
 241  GAGCTCCACCAGAATCCTGGCGTCCAAAACGGCGCGCAAAATCTTTGACGATTCAGAGGA   300
 301  TCAGACAAAAGCTAGGAAAGGAGCTGTGGAGGAGGAGCCTCTTCTGAAGGACAACCCCCA   360
 361  CCGCTTTGTCATTTTTCCAATTCAGTACCATGACATCTGGCAGATGTACAAAAAGGCAGA   420
 421  GGCCTCCTTCTGGACTGCAGAGGAGGTTGACCTGTCCAAAGATCTTCAGCACTGGGATTC   480
 481  CCTGAAAGACGAGGAGAGATATTTCATCTCTCATGTCTTGGCTTTCTTTGCTGCAAGTGA   540
 541  TGGCATTGTCAATGAGAACTTGGTGGAGCGATTTACTCAGGAGGTCCAAGTGACTGAAGC   600
 601  CCGTTGCTTCTACGGTTTCCAGATTGCCATGGAAAACATACACTCTGAAATGTACAGTCT   660
 661  GTTGATTGACACCTATATCAAAGATCCCAAAGAGAGAGATTTTCTTTTCAATGCCATTGA   720
 721  GACAATGCCTTGTGTAAAGAAGAAGGCTGACTGGGCGCTCAACTGGATTGGTGACAAAAA   780
 781  TGCACAATACGGGGAGAGAGTGGTTGCTTTTGCTGCTGTGGAAGGAATCTTCTTTTCTGG   840
 841  GTCTTTTGCTTCTATTTTCTGGCTAAAGAAGAGAGGACTCATGCCTGGACTCACCTTCTC   900
 901  CAATGAACTTATCAGCAGAGATGAGGGTCTTCATTGTGACTTTGCCTGCCTCATGTTCAA   960
 961  GCACTTGGTCAACAAACCTTCAGAAGAAACTGTAAAGAAATAATTGTGAATGCAGTTGC   1020
1021  AATTGAACAGGAATTCCTGACCGATGCTCTGCCAGTAAAGCTTATTGGTATGAATTGTGA   1080
1081  CCTGATGAAGCAATACATTGAATTTGTGGCTGACAGACTTCTGCTTGAGCTGGGATTTGA   1140
1141  CAAGGTTTATAAAGTGGAAAATCCTTTTGACTTCATGGAGAACATTTCCTTGGAGGGCAA   1200
1201  GACCAACTTCTTTGAGAAGAGAGTTGGCGAGTACCAGCGGATGGGAGTCATGTCCGGATC   1260
1261  CACAGATAACACTTTCAGACTGGATGCTGATTTTTAGGGACTCAATCAGCGTGCCTGAAT   1320
1321  GGACACTTAAACGCTTTGGACTCAGGGGTTTTAACCTCACTAATTTCTAGGTTGTTTACA   1380
1381  TGAGTTTTTTTTTTTAAATATAAATACTTTTGCTTCTTTTCAAAGATCTGATATTGAAGT   1440
1441  GCTTTTTGTTTTAAATGATAATAAAAAGAACCAATCTAAAAAAAAAAAAAAAAAAAAA     1496
```

p53R2.1 cDNA

```
   1   GAAAACAAGAGCTAACTCAATGACAGACGACGCAGAGAGACCGCTGCTGACCAAAGACGA      60
  61   ATATAACCGTGAACTCCGGTCTAAGACACACTCTGGCGAACATTATGGAATATCAGAACG     120
 121   GTCACAGGCATGTTGACACAAACAGTGTTGAAGACGAACCCCTTCTCAGAGAAAACCCAA     180
 181   AGCGATTTGTCATTTTCCCTATTCAGTATCCTGACATCTGGAAAATGTACAAACAAGCCC     240
 241   AGGCTTCATTCTGGACAGTCGAGGAGGTGGATTTATCAAAGGACTTGGTTCACTGGGACA     300
 301   GCCTAAAGTCTGAAGAGAAACACTTCATATCCCATGTACTTGCTTTCTTTGCAGCAAGTG     360
 361   ATGGGATAGTCAACGAGAACCTGGTGCAGCGGTTCAGTCAAGAGGTGCAGATCCCAGAAG     420
 421   CTCGCTCCTTCTACGGCTTTCAGATCCTCATAGAGAACGTGCACTCCGAAATGTACAGCA     480
 481   TGCTTATCAACACCTACATAAGGGATCTAAAAGAGAGGGACTATTTGTTTAATGCAATTC     540
 541   ACACCATGCCTTGTGTAAGGCGAAAAGCAGACTGGGCCTTACAGTGGATCTCTGACACAA     600
 601   ACTCAACTTTTGGAGAGCGATTAGTAGCATTTGCAGCAGTGGAAGGCATCTTCTTCTCTG     660
 661   GATCCTTTGCTGCCATCTACTGGTTGAAGAAAAGAGGCCTGATGGCTGGACTCACCTACT     720
 721   CCAATGAACTCATCAGCAGAGATGAGGGTCTGCACTGTAATTTCGCATGTCTATTGTACA     780
 781   GCTACTTGGTGAAGAAACCATCTGCTGACCGAGTGAAAGACATCATCACAAAAGCTGTGA     840
 841   GCATCGAACAGGAGTTTCTCACAGAAGCCTTACCCGTCAATTTGATCGGGATGAACTGCT     900
 901   CTCTCATGAAGCAATACATTGAGTTTGTGGCAGACCGGCTGCTAATGGACCTA**GGATTGC**     960
 961   **CCAAAGTTTTCAAGTCAGAAAACCCTTTCGACTTTATGGAGTCGATTTCATTGGAGGGAA**    1020
1021   **AAACGAATTTTTTCGAGAAGCGGGTGGGTGAATACCAACGACTTGGAGTGATGTCAAATG**    1080
1081   **TGATGGACTGTGAATTCACTCTCGATGCAGATTTC**TAA**CGATGAACTAGAAGAAATATTA**    1140
1141   **TTTATTTTTCGGGACAGTTTCATT**ATTTTATTTTATTTTTTTTTATTGTTTTGCTTTTAAC    1200
1201   TCCAAGAAGAAAGTAAACGATAAACTGTAGACTTTTTAGGTTTCGTTTTATTTTGGTTTC    1260
1261   TTTTTTGTAAAACTTCCAGAACTTCCAAGATGTTTTAGATATTTTTACAATTTACTTGAT    1320
1321   TACTGTACCTAAGTATTGTTTTGGGGGATTTGTTCTTCACGCAAGTGCAATTTAAACTGA    1380
1381   CTACTTGTAATTTTACTTGATTACATTTGTGACCCTGGTCAGTCAAGTGTCAATTTTTTT    1440
1441   AAATTTAGATGTATACATCATCTGAAAGCTGAATAAATATGGTTTCCATTGAAAAAAAAA    1500
1501   AAAAAAA                                                          1507
```

p53R2.1 (alternative splice variant) cDNA

```
   1   GACGCAGAGAGACCGCTGCTGACCAAAGACGAATATAACCGTGAACTCCGGTCTAAGACA      60
  61   CACTCTGGCGAACATTATGGAATATCAGAACGGTCACAGGCATGTTGACACAAACAGTGT     120
 121   TGAAGACGAACCCCTTCTCAGAGAAAACCCAAAGCGATTTGTCATTTTCCCTATTCAGTA     180
 181   TCCTGACATCTGGAAAATGTACAAACAAGCCCA**GGCTTCATTCTGGACAGTCGAGGAGGT**     240
 241   **GGATTTATCAAAGGACTTGGTTCACTGGGACAGCCTAAAGTCTGAAGAGAAACACTTCAT**     300
 301   **ATCCCATGTACTTGCTTTCTTTGCAGCAAGTGATGGGATAGTCAACGAGAACCTGG**CAAG     360
 361   TGCATCTCCTAATGGAAAATTTCAGACTGAGTTGATCAAGAAGTTATTTCCAAACATCAT     420
 421   GTCTTGACTTGTCACAGGTGCAGCGGTTCAGTCAAGAGGTGCAGATCCCAGAAGCTCGCT     480
 481   CCTTCTACGGCTTTCAGATCCTCATAGAGAACGTGCACTCCGAAATGTACAGCATGCTTA     540
 541   TCAACACCTACATAAGGGATCTAAAAGAGAGGGACTATTTGTTTAATGCAATTCACACCA     600
 601   TGCCTTGTGTAAGGCGAAAAGCAGACTGGGCCTTACAGTGGATCTCTGACACAAACTCAA     660
 661   CTTTTGGAGAGCGATTAGTAGCATTTGCAGCAGTGGAAGGCATCTTCTTCTCTGGATCCT     720
 721   TTGCTGCCATCTACTGGTTGAAGAAAAGAGGCCTGATGGCTGGACTCACCTACTCCAATG     780
 781   AACTCATCAGCAGAGATGAGGGTCTGCACTGTAATTTCGCATGTCTATTGTACAGCTACT     840
 841   TGGTGAAGAAACCATCTGCTGACCGAGTGAAAGACATCATCACAAAAGCTGTGAGCATCG     900
 901   AACAGGAGTTTCTCACAGAAGCCTTACCCGTCAATTTGATCGGGATGAACTGCTCTCTCA     960
 961   TGAAGCAATACATTGAGTTTGTGGC                                        985
```

The sequence of the additional intron is underlined. The complete sequence of the 3'-end of this transcript was not obtained.

p53R2.2 cDNA

```
   1    GAGTGGAGGAGGAGCTATAGTATGAGCGTGTTGTAAATGACAGACGACAGAGAGATCGCA     60
  61    GCTCTACCGCTGCTGACCAAAGACGATTATAACCATGAACTCCAGCACAAGCAACACTCT    120
 121    GTCGAGCGTTATGGAATATCAGAATGGTCACAAGGATGTTGACGCAAACAGTGTTGAAGA    180
 181    CGAACCCCTTCTCAAAGAAAACCCAAAGCGATTTGTAATTTTTCCGATTCAGTATCCCGA    240
 241    CATCTGGAAAATGTACAAACAAGCCCAGGCGTCATTTTGGACAGTTGAGGAGGTGGATTT    300
 301    ATCAAAGGACTTGGTCCACTGGGACAGCCTGAAGTCTGAAGAGAAACACTTCATATCCCA    360
 361    TGTACTGGCTTTCTTTGCAGCAAGTGATGGGATAGTCAACGAGAACCTGGTGCAGCGGTT    420
 421    CAGTCAAGAGGTGCAGATCCCAGAGGCTCGCTCCTTCTACGGCTTTCAGATCCTCATAGA    480
 481    GAATGTGCACTCCGAAATGTACAGCATGCTCATCAACACCTACATAAGGGATCTGAAAGA    540
 541    GAGGGACTTTTTGTTCAATGCAATTCACACCATGCCTTTTGTAAGGCGGAAAGCAGACTG    600
 601    GGCCTTACAGTGGATCTCTGACACAAACTCAACTTTTGGAGAACGATTAGTAGCATTTGC    660
 661    AGCAGTGGAAGGCATCTTCTTCTCTGGATCATTTGCGGCCATCTACTGGTTGAAGAAAAG    720
 721    AGGCCTGATGCCAGGACTCACTTACTCCAATGAACTCATCAGCAGAGATGAGGGTCTGCA    780
 781    CTGTAATTTTGCATGTCTAATGTACAGCTACTTGGTGAAGAAACCTTCTGCTGACCGAGT    840
 841    GAAAGACATCATCACAAAAGCTGTGAGCATTGAACAGGAGTTTCTCACAGAAGCCTTACC    900
 901    CGTCAATTTGATCGGGATGAACTGCTCTCTCATGAAGCAGTACATTGAGTTTGTGGCTGA    960
 961    CCGGCTGCTAACAGACTTAGGATTGCCCAAAGTTTACAAGTCAGAAAACCCCTTCGACTT   1020
1021    CATGGAGTCCATTTCATTGGAGGGAAAAACTAATTTCTTCGAGAAGCGAGTGGCTGAATA   1080
1081    CCAGCGACTTGGAGTGATGTCAAATGTGATGGACTGTGAATTCACTCTTGATGCAGATTT   1140
1141    CTAACGATGAACTACAAGAAATATTATTTATTTTTTGGGACAGTTTCAGTAAAAACAAA   1200
1201    CAAAAAACAAGCCATATCACCTTCAGACCTTGTCGAAAAGAAAGTGGAAATCAGGTTTA   1260
1261    CCAGTTTCTGAATAACATGGTAACGAATTTGTCAAAGAGCTCACCAAAGTGGACGTGTGG   1320
1321    CTTTAGCGTATTCAGACCAGACTTGGTGTGTGTTATGACAACCATTATCTGAGGTTGCAT   1380
1381    GCACAGTTTCGACATACTGCCACCACTGGTCAGGAGATATGAAAAA              1426
```